Structural investigation of Fe(III)-salen complexes as "turn-on" fluorogenic probes for selective detection of pyrophosphate ions

Eunice Y.-L. Hui, Dillon W.P. Tay, Jean-Alexandre Richard, Zuzana Pohancenikova, Kevin Renault, Anthony Romieu, Yee Hwee Lim

Structural investigation of Fe(III)-salen complexes as "turn-on" fluorogenic probes for selective detection of pyrophosphate ions

Eunice Y.-L. Hui[a], Dillon W. P. Tay[a], Jean-Alexandre Richard[a,1], Zuzana Pohancenikova[b], Kevin Renault[b,2], Anthony Romieu[b,*], Yee Hwee Lim[a,*]

[a]*Institute of Sustainability for Chemicals, Energy and Environment, Agency for Science, Technology & Research, 8 Biomedical Grove, #07-01 Neuros Building, Singapore 138655*
[b]*Institut de Chimie Moléculaire de l'Université de Bourgogne, UMR 6302, CNRS, Univ. Bourgogne Franche-Comté, 9, Avenue Alain Savary, 21000 Dijon, France*

[1]Present address: Research and Technology Development, Illumina, 29 Woodlands Industrial Park E1, 757716 Singapore
[2]Present address: Département de Chimie, Laboratoire de Chimie Bio-Organique, University of Namur (FUNDP), Rue de Bruxelles 61, 5000 Namur, Belgium

Graphical abstract

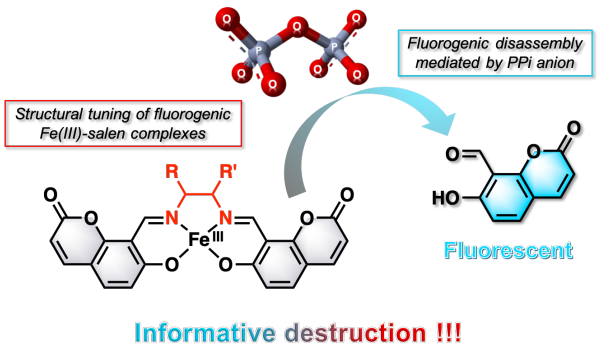

ABSTRACT

In this work, we revisited the disassembly approach (also known as the Zelder's approach) recently proposed for sensing pyrophosphate (PPi) in water and based on the decomposition of metal-salen complexes. A systematic study devoted to the structural optimization of this novel class of PPi-responsive fluorogenic probes was conducted. Screening of eight different vicinal diamines (*i.e.*, bridge of the salen ligand) combined with the use of 8-formyl-7-hydroxycoumarin (*i.e.*, salicylaldehyde derivative) as the fluorescent reporter, has led to a set of novel and fully characterized coumarin-salen Fe(III) complexes. A series of analytical validations helped us to identify that coumarin-salen Fe(III) complexes derived from ethylenediamine and racemic 1,2-propylenediamine backbones exhibit the best and selective PPi-sensing performances (the limits of detection were estimated as 3.15×10^{-6} M and 2.81×10^{-6} M respectively). The implementation of both fluorescence time-course measurements and RP-HPLC-fluorescence analyses has enabled us to gain further insights into the disassembly-based probes' activation mechanism. This study therefore contributes to demonstrate that the disassembly approach is a valuable strategy to achieve fluorogenic activity-based sensing of anions.

* Corresponding authors. Phone (A. R.) +33 3 80 39 36 24; e-mail anthony.romieu@u-bourgogne.fr, or Phone (Y. H. L.) +65 6799 8508; e-mail lim_yee_hwee@isce2.a-star.edu.sg

Keywords Disassembly approach; Fluorogenic probe; Turn-on detection; Pyrophosphate ion; Salen ligand

Highlights

A series of coumarin-salen Fe(III) complexes with various diamine bridges were synthesized

Coumarin-salen Fe(III) complexes were used to detect pyrophosphate (PPi) through a fluorogenic disassembly approach

Fe(III) complexes with ethylene- and 1,2-propylenediamine bridges offered the best performances

Fe(III) complex with 1,2-propylenediamine bridge showed good selectivity and a limit of detection of 2.81×10^{-6} M

Disassembly mechanism was deciphered by NMR and RP-HPLC-fluorescence analyses

1. Introduction

Inorganic pyrophosphate (PPi) plays a vital role in various biological processes. It is involved in physiological pathways associated with energy storage [1], ion-channel regulation [2], iron delivery [3], telomere maintenance [4] and cell signaling [5]. PPi is also released as a byproduct from polymerase-catalyzed synthesis of nucleic acids (DNA or RNA) [6] and can thus be leveraged to gauge oligonucleotide polymerization progress. Since oligonucleotide therapeutics have recently emerged as a promising drug modality [7], it is anticipated that there will be a growing need for analytical tools for PPi detection serving as reaction progress indicators to provide cost and safety benefits for oligonucleotide manufacturing processes based on enzymatic synthesis [8,9]. With respect to PPi detection, the use of fluorescent and colorimetric probes has promoted the emergence of rapid and sensitive sensing approaches scalable for high throughput screening applications [10]. Typically, these PPi-responsive probes have binding sites designed to specifically interact with this anion through hydrogen bonding [11] or ionic interactions [12] that trigger an optical response *via* a covalently attached fluorescent or colorimetric tag. These probes are able to transduce PPi detection events into a signal response through various photophysical mechanisms [13] such as chelation enhanced fluorescence (CHEF), internal charge transfer (ICT), excimer formation, aggregation-induced emission (AIE), aggregation-caused quenching (ACQ), photoinduced electron transfer (PeT) or excited-state intramolecular proton transfer (ESIPT). Recently, an alternative sensing approach combining the well-known displacement assay (*i.e.*, displacement of the metal cation upon PPi binding) [10,14] to a ligand hydrolysis reaction, has been developed. Thus, Zelder and co-workers pioneered metal-salen-based probes that detect PPi anions *via* a "turn-on" fluorogenic response arising from a molecular disassembly process that releases fluorescent salicylaldehyde [15-19],[20] (Fig. 1). The displacement of the chelated metal that subsequently triggers disassembly of the salen ligand, is promoted by strong metal cation-pyrophosphate interaction and subsequent precipitation of the metal pyrophosphate salt in aqueous media. A similar strategy based on rapid hydrolysis of an imine-functionalized "turn-on" fluorophore in water has been reported by Kim and co-workers for the detection of cyanides through Cu(II) displacement and subsequent release of a green-emissive 7-(dialkylamino)coumarin-3-carbaldehyde [21]. The Zn(II)-salen complex initially developed by Zelder and co-workers exhibited subdued performances due primarily to

stability issues in aqueous media, limited sensitivity and poor selectivity between polyphosphate species [15]. A later iteration with harder Lewis acid Fe(III) as the metal cation imparted enhanced aqueous stability and better quenching of intrinsic salen ligand fluorescence, thus allowing a "turn-on" fluorogenic detection mechanism [16]. It has also been demonstrated that introducing substituents on the bis-imine backbone of the salen ligand can tune selectivity behavior of the corresponding Fe(III)-salen based complexes (Fig. 2). Replacing the original ethylenediamine bridge with another vicinal diamine had dramatic effects on probe selectivity between PPi and adenosine triphosphate (ATP). Poorer selectivity was obtained with 2,3-diaminobutanedinitrile. By contrast, 2,3-diaminopropane has enabled improved selectivity whereas *ortho*-phenylenediamine led to an Fe(III)-salen complex which was unable to detect polyphosphate species [16].

Being heavily interested in this disassembly strategy for PPi fluorogenic sensing, we rationalized that replacing the salicylaldehyde signaling unit (known to be a poor fluorophore [22], relative fluorescence quantum yield lower than 0.3% determined in the conditions of our study: HEPES buffer, 20 mM, pH 7.3, see Fig. S63 for the corresponding UV-visible absorption and fluorescence spectra) of the Fe(III)-salen complex with brighter fluorophores bearing an *ortho*-hydroxybenzaldehyde moiety could boost sensitivity and provide next-generation PPi-sensitive probes with higher performances. This approach is complementary to that intensively studied by the Zelder group and based on changes in substitution pattern of the salicylaldehyde molecule to enhance both its fluorescence properties and overall aqueous solubility of Fe(III)-salen complexes [17]. In addition to the work focused on fluorescent reporter, it may be also interesting to consider further tuning of steric and electronic properties of the bis-imine bridge aimed at improving selectivity for PPi anions. In this context, we report herein the synthesis and characterization of a series of Fe(III)-salen complexes derived from 8-formyl-7-hydroxycoumarin [23] and bearing a bis-imine bridge decorated with various substituents (Fig. 2). Interestingly, various coumarin-salen metal complexes derived from this fluorescent *ortho*-salicylaldehyde derivative have already been studied, thus highlighting some attractive properties often correlated with the nature of chelated metal: antibacterial/antifungal and antioxidant activities [24-26], DNA cleavage ability [24,25], binding ability to DNA G-quadruplexes [27,28], and catalytic activity for solvent-free ring-opening polymerization (ROP) of ε-caprolactone [29], but they have never been used for fluorogenic anion sensing purposes. Systematic structural alteration of the bis-imine bridge

with various substituents (Me, Ph, CF_3, iPr) or elongation of the linker length (from two to three carbon atoms) was achieved and the spectral properties of their corresponding Fe(III) complexes characterized. Probe selectivity to a variety of anions including multiple polyphosphate species were quantified and compared to evaluate the impact of bis-imine bridge modification on this key feature. In addition to this optimization work devoted to PPi sensing performance, a set of *in vitro* fluorescence assays, HPLC-fluorescence and NMR analyses was undertaken to study in detail the PPi-mediated disassembly mechanism of such Fe(III)-salen complexes.

2. Experimental section

2.1. General

All reactions were performed under an argon atmosphere; they were carried out at room temperature (RT, 25 °C) unless stated otherwise. Chemicals and solvents were either analytical reagent grade or purified by standard techniques (*e.g.*, salicylaldehyde purchased from Janssen Chimica (98%, #13.260.68) was purified by distillation). 7-Hydroxycoumarin (98%, #L04082) used as a standard for the determination of relative fluorescence quantum yields, was purchased from Alfa Aesar. Preparative TLC purifications were performed on Supelco TLC silica gel 60G F_{254} glass plates (#1.00390, 20×20 cm). The bands were visualized through illumination with single wavelength UV lamp (λ = 254 nm). Molecular biology and UV-spectroscopy grade DMSO were provided by Sigma-Aldrich (#D8418) and Honeywell Riedel-de-Haën (#41641) respectively. The HPLC-gradient grade MeCN was obtained from Carlo Erba or Fisher Scientific. HEPES buffer (20 mM, pH 7.2 or 7.35) and aq. mobile-phases for HPLC were prepared using ultrapure water produced by an ELGA PURELAB Ultra system (purified to 18.2 MΩ.cm). TEAA buffer (2.0 M, pH 7.0) was prepared from distilled TEA and glacial AcOH.

2.2. Instruments and methods

^{1}H, ^{13}C and ^{19}F NMR spectra were recorded on a Bruker Avance 400 MHz spectrometer. Chemical shifts (δ) were reported in ppm and residual non-deuterated solvent peaks were used as internal reference (proton δ = 7.26 and carbon δ = 77.16 for $CDCl_3$, proton δ = 2.50 and carbon δ = 39.52 for DMSO-d_6, and proton δ = 3.31 and carbon δ = 49.00 for CD_3OD) [30].

No internal standard was used for $^{19}F\{^{1}H\}$ NMR. ^{1}H NMR coupling constants (*J*) are reported in Hertz (Hz). The following abbreviations were used in reporting multiplicities: s (singlet), d (doublet), t (triplet), m (multiplet), dd (doublet of doublets), ddd (doublet of doublet of doublets), qd (quartet of doublets) and td (triplet of doublets). IR spectra were recorded with a PerkinElmer Spectrum 100 FT-IR spectrometer fitted with attenuated total reflectance (ATR) accessory. The bond vibration frequencies are expressed in wavenumbers (cm^{-1}). High-resolution mass spectra (HRMS) were recorded on an Agilent ESI-TOF mass spectrometer at 3.5 kV emitter voltage. Exact *m/z* values are reported in Daltons. RP-HPLC analyses (UV-visible or fluorescence detection) were performed on a Thermo-Dionex Ultimate 3000 instrument (pump + autosampler at 20 °C + column oven at 25 °C) equipped with a diode array detector (Thermo-Dionex DAD-3000RS) and a fluorescence detector (Thermo-Dionex FLD-3400RS with dual PMT 200-900 nm). The chromatographic system detailed below, was used for these analyses. *System A*: RP-HPLC-fluorescence (Phenomenex Kinetex C_{18} column, 2.6 µm, 2.1 × 50 mm) with MeCN and aq. TEAA (25 mM, pH 7.0) as eluents [5% MeCN (0.1 min) followed by linear gradient from 5% to 100% (5 min) of MeCN, then 100% MeCN (3 min)] at a flow rate of 0.5 mL/min. Fluorescence detection was achieved at 45 °C at the following Ex/Em channel: 365/495 nm (sensitivity: 1, PMT Auto, filter wheel: Auto). All spectral measurements (UV-visible absorbance and fluorescence emission) made in Singapore ($ISCE^2$, A*STAR) were performed with a PerkinElmer 2104 EnVision Multilabel Plate Reader. UV-visible spectra were recorded between 300 and 700 nm at 1 nm resolution. Ex/Em bandwidths for fluorescence measurements were kept at 8 nm; Ex wavelength was set at 365 nm. For spectral measurements made in Dijon (ICMUB, University of Burgundy), the instruments listed below, have been used. UV-visible spectra were obtained either on a Varian Cary 50 Scan (single-beam, software Cary WinUV) or on a SAFAS $UVmc^2$ (dual-beam, software SP2000 version 7.8.13.0) spectrophotometer by using a rectangular quartz cell (Hellma, 100-QS, 45 × 12.5 × 12.5 mm, pathlength: 10 mm, chamber volume: 3.5 mL), at 25 °C (using a temperature control system combined with water circulation). The absorption spectra of salicylaldehyde, 7-hydroxycoumarin derivatives and salen ligands were recorded in HEPES buffer within the concentration range 1-80 µM (three distinct dilutions for the accurate determination of molar extinction coefficients of novel compounds). The vast majority of fluorescence spectra were recorded on an HORIBA Jobin Yvon Fluorolog spectrofluorometer (software FluorEssence) at 25 °C (using a temperature control system

combined with water circulation), with a standard fluorometer cell (Labbox, LB Q, light path: 10 mm, width: 10 mm, chamber volume: 3.5 mL). The following set of parameters was used: shutter: Auto Open, Ex/Em slits = 5 nm for recording emission spectra and Ex/Em slits = 5 nm for recording excitation spectra, integration time = 0.1 s, 1 nm step, HV(S1) = 950 V. All fluorescence spectra were corrected. Relative fluorescence quantum yields were measured in HEPES buffer at 25 °C by a relative method using the suitable standard (7-hydroxycoumarin: Φ_F = 76% in PB (100 mM, pH 7.4), excitation at 340 nm; dilution by a factor ×10 between absorption and fluorescence measurements) [31]. The following equation was used to determine the relative fluorescence quantum yield:

$$\Phi_F(x) = (A_S/A_X)(F_X/F_S)(n_X/n_S)^2\Phi_F(s)$$

where A is the absorbance (in the range of 0.01-0.1 A.U.), F is the area under the emission curve, n is the refractive index of the solvents (at 25 °C) used in measurements, and the subscripts s and x represent standard and unknown, respectively. The following refractive indices was used for PB and HEPES buffer: 1.337. Fluorescence-based kinetic assays were performed on a SAFAS Flx-Xenius XC spectrofluorimeter using quartz cells (SAFAS, Quartz Suprasil for SAFAS flx Xenius, 45 × 12.5 × 12.5 mm, pathlength: 10 mm, chamber volume: 3.5 mL), at 25 °C (using a temperature control system combined with water circulation). The following set of parameters was used: Ex/Em 365/495 nm, Ex/Em bandwidths = 5 nm, PMT voltage = 600 V.

2.3. Synthesized compounds

8-Formyl-7-hydroxycoumarin *[2067-86-9]*. 7-Hydroxycoumarin (243 mg, 1.50 mmol, 1 equiv.) and hexamine (484 mg, 3.45 mmol, 2.3 equiv.) were dissolved in TFA (10 mL) and the resulting reaction mixture was stirred at 80 °C for 3 days. Then, aq. HCl (1.0 M, 10 mL) was added and the mixture was stirred at RT for 3 h. Afterwards, the reaction mixture was diluted with EtOAc (20 mL) and washed with brine (20 mL). Organic layer was dried over anhydrous Na_2SO_4 and concentrated under reduced pressure. The crude product was dissolved in minimal amount of EtOH and precipitated using deionized water to provide the salicylaldehyde derivative as a pale yellow solid (285 mg, yield 41%). ^{1}H NMR (400 MHz, $CDCl_3$):

δ = 10.61 (d, *J* = 0.6 Hz, 1H), 7.69 (d, *J* = 9.6 Hz, 1H), 7.61 (d, *J* = 8.8 Hz, 1H), 6.93-6.87 (m, 1H), 6.36 (d, *J* = 9.6 Hz, 1H); LRMS (ESI^-, recorded during RP-HPLC analysis, system S1): *m/z* 189.1 $[M - H]^-$ (100), calcd for $C_{10}H_5O_4^-$ 189.0; HRMS (ESI+): *m/z* calcd for $C_{10}H_6O_4Na^+$ $[M + Na]^+$ 213.0158, found 213.0151. All other spectroscopic data are identical to those reported by Skarga *et al*. [32].

Neutralization of vicinal diamine dihydrochloride salts. Commercial vicinal diamine dihydrochloride (1 equiv.) and NaOH (2.2 equiv.) was dissolved in deionized water (1 mL). The mixture was stirred at RT for 1 h and then adjusted to pH 7 with aq. HCl solution (6.0 M). Acetone (10 mL) was added and the mixture was centrifuged for 7 min (4000 rpm) to remove the solids. Acetone was removed using rotary evaporator and EtOH (10 mL) was then added. The desired free base diamine was evaporated to dryness and used for salen ligand formation. Other vicinal diamines (1,2-ethylenediamine, 1,3-diaminopropane, 1,2-propylenediamine and 1,2-diphenylethylenediamine) are commercially available directly as free base form.

General procedure A for salen ligand formation. Vicinal diamine (1 equiv.) in EtOH (3 mL) was added dropwise to 8-formyl-7-hydroxycoumarin (2 equiv.) in EtOH (7 mL) at 25 °C. The resulting reaction mixture was stirred at 50 °C for 3 h and left to stand in 4 °C fridge overnight. The precipitate formed was filtered and washed with EtOH (×2) and Et_2O (×1) to furnish the desired salen ligand.

General procedure B for salen ligand formation. Vicinal diamine (1 equiv.) dissolved in a mixture of EtOH and DMF (10 : 1, v/v) was added dropwise to 8-formyl-7-hydroxycoumarin (2 equiv.) and *para*-toluenesulfonic acid (PTSA, 0.01 equiv.) in EtOH (7 mL). The resulting reaction mixture was stirred at 80 °C for 16 h and left to stand in 4 °C fridge overnight. The precipitate formed was filtered and washed with EtOH (×2) and Et_2O (×1) to furnish the desired salen ligand.

Synthesized salen ligands

Salen ligand based on 1,2-ethylenediamine [1644074-63-4] ***1-L*** *[33,34]:* synthesized according to procedure A and using 1,2-ethylenediamine. Yellow solid (76 mg, yield 72%). IR (ATR): ν_{max} = 1718, 1629 (C=N), 1582, 1510, 1435, 1237, 1186, 1107, 989, 831, 773; ^1H NMR

(400 MHz, DMSO-d_6): δ = 8.96 (s, 2H), 7.87 (d, *J* = 9.4 Hz, 2H), 7.53 (d, *J* = 9.1 Hz, 2H), 6.58 (d, *J* = 9.0 Hz, 2H), 6.12 (d, *J* = 9.4 Hz, 2H), 4.08 (s, 4H); ^{13}C NMR (101 MHz, DMSO-d_6): δ = 174.1, 161.8, 160.2, 156.6, 145.7, 134.4, 118.7, 109.4, 107.2, 104.6, 54.0; LRMS (ESI+, recorded during RP-HPLC analysis, system S1): *m/z* 405.1 $[M + H]^+$ (100), calcd for $C_{22}H_{17}N_2O_6^+$ 405.1; HRMS (ESI+): *m/z* calcd for $C_{22}H_{17}N_2O_6^+$ $[M + H]^+$ 405.1081, found 405.1071; UV (HEPES buffer, pH 7.3, 25 °C): λ_{max} = 281 nm (ε 25 350 M^{-1} cm^{-1}), 349 nm (ε 33 800 M^{-1} cm^{-1}).

*Salen ligand based on 1,3-diaminopropane **2-L**:* synthesized according to procedure A and using 1,3-diaminopropane. Yellow solid (82 mg, yield 37% yield); IR (ATR): ν_{max} = 1715, 1634 (C=N),1582, 1511, 1431, 1253, 1183, 1109, 833, 774; ^{1}H NMR (400 MHz, DMSO-d_6): δ = 8.89 (s, 2H), 7.81 (d, *J* = 9.4 Hz, 2H), 7.45 (d, *J* = 9.1 Hz, 2H), 6.47 (d, *J* = 9.1 Hz, 2H), 6.05 (d, *J* = 9.4 Hz, 2H), 3.84 (t, *J* = 6.6 Hz, 4H), 2.13 (t, *J* = 6.7 Hz, 2H); ^{13}C NMR (101 MHz, DMSO-d_6): δ = 175.5, 160.8, 160.3, 156.8, 145.6, 134.4, 119.2, 108.8, 106.5, 104.3, 51.2, 30.5; HRMS (ESI+): *m/z* calcd for $C_{23}H_{18}N_2O_6Na$ $[M + Na]^+$ 441.1057, found 441.1047.

*Salen ligand based on racemic 1,2-propylenediamine **3-L**:* synthesized according to procedure A and using racemic 1,2-propylenediamine. Yellow solid (60 mg, yield 55%). IR (ATR): ν_{max} = 1720, 1627 (C=N), 1583, 1511, 1314, 1236, 1189, 1108, 988, 832, 773; ^{1}H NMR (400 MHz, DMSO-d_6): δ = 8.98 (d, *J* = 12.2 Hz, 2H), 7.89 (dd, *J* = 12.7, 9.5 Hz, 2H), 7.56 (dd, *J* = 17.3, *J* = 9.0 Hz, 2H), 6.66 (d, *J* = 9.0 Hz, 1H), 6.58 (d, *J* = 9.0 Hz, 1H), 6.15 (dd, *J* = 14.9, *J* = 9.4 Hz, 2H), 4.25-4.16 (m, 1H), 4.04 (qd, *J* = 12.9, *J* = 5.9 Hz, 2H), 1.39 (d, *J* = 6.5 Hz, 3H); ^{13}C NMR (101 MHz, DMSO-d_6): δ = 173.4, 171.5, 161.4(d), 159.8, 159.6, 159.5, 156.0, 155.6, 145.1(t), 133.9(d), 133.6(d), 118.0, 117.2, 109.6(d), 109.0(d), 107.6, 106.8, 104.30, 104.1, 60.4, 58.7, 18.8; LRMS (ESI+, recorded during RP-HPLC analysis, system S1): *m/z* 419.1 $[M + H]^+$ (100), calcd for $C_{23}H_{19}N_2O_6^+$ 419.1; LRMS (ESI-, recorded during RP-HPLC analysis): *m/z* 417.1 $[M - H]^-$ (100), calcd for $C_{23}H_{17}N_2O_6^-$ 417.1; HRMS (ESI+): *m/z* calcd for $C_{23}H_{19}N_2O_6^+$ $[M + H]^+$ 419.1238, found 419.1230; UV (HEPES buffer, pH 7.3, 25 °C): λ_{max} = 282 nm (ε 23 200 M^{-1} cm^{-1}), 349 nm (ε 27 700 M^{-1} cm^{-1}).

*Salen ligand based on racemic 2,3-diaminobutane **4-L**:* synthesized according to procedure B and using racemic 2,3-diaminobutane. Yellow solid (61 mg, yield 54% yield). IR (ATR): ν_{max} = 1722, 1627 (C=N), 1594, 1512, 1238, 1114, 1003, 984, 914, 827, 774; ^{1}H NMR (400 MHz,

DMSO-d_6): δ = 14.94 (s, 2H, O*H*), 9.05 (d, *J* = 5.5 Hz, 2H), 7.93 (d, *J* = 9.5 Hz, 2H), 7.61 (d, *J* = 9.0 Hz, 2H), 6.67 (d, *J* = 8.9 Hz, 2H), 6.20 (s, 2H), 4.13 (s, 2H), 1.36 (d, *J* = 6.2 Hz, 6H); ^{13}C NMR (101 MHz, DMSO-d_6): δ = 171.9, 160.4, 160.1, 156.0, 145.6, 134.1, 117.6, 110.2, 108.2, 105.0, 64.5, 17.5; HRMS (ESI+): *m/z* calcd for $C_{24}H_{21}N_2O_6^+$ $[M + H]^+$ 433.1394, found 433.1388.

Salen ligand based on racemic 3,3,3-trifluoro-1,2-diaminopropane ***5-L****:* synthesized according to procedure B and using racemic 3,3,3-trifluoro-1,2-diaminopropane. Further purification by preparative TLC (eluent: CH_2Cl_2-MeOH 9:1 v/v) provided salen ligand **5-L** as yellow film (19 mg, yield 15%). ^{1}H NMR (400 MHz, CD_3OD): δ = 9.08 (s, 1H), 8.88 (s, 1H), 7.73 (d, *J* = 9.6 Hz, 1H), 7.66 (d, *J* = 9.5 Hz, 1H), 7.51 (d, *J* = 8.8 Hz, 1H), 7.38 (d, *J* = 9.0 Hz, 1H), 6.78 (d, *J* = 8.8 Hz, 1H), 6.59 (d, *J* = 8.9 Hz, 1H), 6.13 (d, *J* = 9.5 Hz, 1H), 6.03 (d, *J* = 9.4 Hz, 1H), 4.52 (td, *J* = 7.1, 3.8 Hz, 1H), 4.26 (dd, *J* = 13.2 Hz, *J* = 4.0 Hz, 1H), 4.08 (dd, *J* = 13.1 Hz, *J* = 7.7 Hz, 1H); ^{13}C NMR (101 MHz, CD_3OD): δ = 172.0, 167.3, 166.3, 164.11, 162.2, 161.7, 156.9, 156.2, 146.2, 145.9, 135.0, 134.8, 123.1, 117.9, 115.7, 113.1, 112.2, 111.5, 110.2, 107.1, 106.4, 70.5, 70.2, 56.2; ^{19}F {^{1}H} NMR (376 MHz, DMSO-d_6): δ = -72.04 (s, 3H, C*F*$_3$); HRMS (ESI+): *m/z* calcd for $C_{23}H_{16}F_3N_2O_6^+$ $[M + H]^+$ 473.0955, found 473.0950. *Note: in pure form, this salen ligand was found to be relatively unstable. Thus, IR and good quality ^{19}F NMR spectra were not obtained. Singlet at -72.04 ppm was assigned via 2D NMR analyses (i.e., carbon-fluorine correlation).*

Salen ligand based on racemic N-phenylethylenediamine ***6-L****:* synthesized according to procedure B and using racemic *N*-phenylethylenediamine. Yellow solid (25 mg, yield 20%). IR (ATR): ν_{max} = 1726, 1627 (C=N), 1589, 1235, 1109, 992, 975, 829, 775; ^{1}H NMR (400 MHz, DMSO-d_6): δ = 14.90 (d, *J* = 3.1 Hz, 1H, O*H*), 14.57-14.40 (m, 1H, O*H*), 9.11 (d, *J* = 3.0 Hz, 1H), 8.97 (d, *J* = 7.4 Hz, 1H), 7.90 (dd, *J* = 31.5 Hz, *J* = 9.5 Hz, 2H), 7.64 (d, *J* = 8.9 Hz, 1H), 7.57-7.50 (m, 3H), 7.46 (dd, *J* = 8.3 Hz, *J* = 6.8 Hz, 2H), 7.39-7.34 (m, 1H), 6.79 (d, *J* = 8.8 Hz, 1H), 6.55 (d, *J* = 9.0 Hz, 1H), 6.22 (d, *J* = 9.5 Hz, 1H), 6.12 (d, *J* = 9.4 Hz, 1H), 5.25 (s, 1H), 4.44-4.36 (m, 1H), 4.35-4.27 (m, 1H); ^{13}C NMR (101 MHz, DMSO-d_6): δ = 173.8, 168.6, 161.9, 161.3, 160.1, 159.9, 156.4, 155.4, 145.6, 145.4, 139.5, 134.4, 134.0, 129.4, 128.6, 127.7, 118.5, 116.1, 111.2, 109.6, 109.5, 107.3, 105.5, 104.6, 70.4, 59.5; HRMS (ESI+): *m/z* calcd for $C_{28}H_{21}N_2O_6^+$ $[M + H]^+$ 481.1394, found 481.1388.

*Salen ligand based on racemic 1,2-diphenylethylenediamine **7-L**:* synthesized according to procedure A and using racemic 1,2-diphenylethylenediamine. Yellow solid (26 mg, yield 18%). IR (ATR): ν_{max} = 1727, 1623 (C=N), 1591, 1493, 1241, 1110, 997, 834, 775, 757, 700; ^{1}H NMR (400 MHz, DMSO-d_6): δ = 9.04 (d, *J* = 2.5 Hz, 2H), 7.87 (d, *J* = 9.5 Hz, 2H), 7.57 (d, *J* = 8.9 Hz, 2H), 7.43-7.39 (m, 4H), 7.29 (t, *J* = 7.5 Hz, 4H), 7.24-7.19 (m, 2H), 6.72 (d, *J* = 8.8 Hz, 2H), 6.18 (d, *J* = 9.5 Hz, 2H), 5.63 (s, 2H); ^{13}C NMR (101 MHz, DMSO-d_6): δ = 168.9, 161.3, 159.8, 155.3, 145.3, 139.0, 133.9, 129.0, 128.4, 128.3, 116.2, 111.2, 109.3, 105.3, 74.9; HRMS (ESI+): *m/z* calcd for $C_{35}H_{27}N_2O_5^+$ $[M + H]^+$ 557.1707, found 557.1699.

*Salen ligand based on racemic 3-methylbutane-1,2-diamine **8-L**:* synthesized according to procedure B and using racemic 3-methylbutane-1,2-diamine. Further purification by preparative TLC (eluent: CH_2Cl_2-MeOH 9:1, v/v) provided salen ligand **8-L** as yellow film (6 mg, yield 3%). *Isolated amount was too small for recording IR spectrum*. ^{1}H NMR (400 MHz, CD_3OD): δ = 8.87 (d, *J* = 15.1 Hz, 2H), 7.72 (dd, *J* = 18.4 Hz, *J* = 9.5 Hz, 2H), 7.44 (dd, *J* = 27.1 Hz, *J* = 9.0 Hz, 2H), 6.70 (d, *J* = 8.9 Hz, 1H), 6.56 (d, *J* = 9.1 Hz, 1H), 6.08 (dd, *J* = 18.5 Hz, *J* = 9.4 Hz, 2H), 4.17 (dd, *J* = 13.1 Hz, *J* = 3.6 Hz, 1H), 4.00 (dd, *J* = 13.1 Hz, *J* = 8.9 Hz, 1H), 3.69 (ddd, *J* = 9.1 Hz, *J* = 5.8 Hz, *J* = 3.5 Hz, 1H), 2.20-2.11 (m, 1H), 1.11 (dd, *J* = 8.4 Hz, *J* = 6.8 Hz, 6H); ^{13}C NMR (101 MHz, CD_3OD): δ = 175.9, 173.2, 163.1, 162.6, 162.4, 162.2, 157.6, 157.0, 146.3, 146.2, 135.6, 135.1, 119.6, 118.4, 111.2, 110.4, 109.9, 108.8, 106.0, 105.7, 73.7, 57.7, 32.0, 19.8, 18.6; HRMS (ESI+): *m/z* calcd for $C_{25}H_{23}N_2O_6^+$ $[M + H]^+$ 447.1551, found 447.1542.

General preparative method for Fe(III) complexes

Salen ligand (1 equiv.) was dissolved in EtOH-H_2O (4:1 v/v, 10 mL) at 50 °C. To this mixture, a solution of $FeCl_3$. $6H_2O$ (1 equiv.) in EtOH (1 mL) was added. The color of the reaction mixture changed from bright yellow to dark violet. It was stirred at 50 °C for 2 h and left to stand in 4 °C fridge overnight. The complex formed was filtered and washed with EtOH (×4) and Et_2O (×1).

Synthesized coumarin-salen Fe(III) complexes

*Fe(III) complex **1-C**:* brick red solid (15 mg, yield 32%); IR (ATR): ν_{max} = 1725, 1614 (C=N), 1585, 1531, 1403, 1324, 1231, 1110, 839, 776, 733; LRMS (ESI+, recorded during RP-HPLC

analysis, system S1): *m/z* 458.0 $[M]^+$ (20), 499.1 $[M + MeCN]^+$ (100), 536.1 $[M + Cl + MeCN + H]^+$ (75), calcd for HRMS (ESI+): *m/z* calcd for $C_{22}H_{14}FeN_2O_6^+$ 458.0; $[M]^+$ 458.0196, found 458.0191; Anal. calcd for $C_{22}H_{18}N_2O_8FeCl$ [M + Cl + $2H_2O$]: C 49.89, H 3.43, N 5.29. Found: C 50.18, H 3.23, N 5.11%; UV (HEPES buffer, pH 7.3, 25 °C): λ_{max} = 353 nm (ε 18 200 M^{-1} cm^{-1}).

*Fe(III) complex **2-C**:* brick red solid (38 mg, yield 56%); IR (ATR): ν_{max} = 1698, 1614 (C=N), 1582, 1528, 1407, 1336, 1232, 1118, 842, 774, 730; HRMS (ESI+): *m/z* calcd for $C_{23}H_{16}FeN_2O_6$ $[M]^+$ 472.0352, found 472.0342; UV (HEPES buffer, pH 7.3): λ_{max} = 358 nm.

*Fe(III) complex **3-C**:* brick red solid (24 mg, yield 43%); IR (ATR): ν_{max} = 1716, 1614 (C=N), 1584, 1529, 1404, 1327, 1231, 1111, 837, 775, 732; LRMS (ESI+, recorded during RP-HPLC analysis, system S1): *m/z* 472.0 $[M]^+$ (100), 513.1 $[M + MeCN]^+$ (100), 550.1 $[M + Cl + MeCN + H]^+$ (100); calcd for $C_{23}H_{16}FeN_2O_6^+$ 472.0; HRMS (ESI+): *m/z* calcd for $C_{23}H_{16}FeN_2O_6^+$ $[M]^+$ 472.0352, found 472.0341; Anal. calcd for $C_{23}H_{18}N_2O_7FeCl$ [M + Cl + H_2O]: C 52.55, H 3.45, N 5.33. Found: C 52.21, H 3.38, N 5.04%; UV (HEPES buffer, pH 7.3, 25 °C): λ_{max} = 359 nm (ε 23 250 M^{-1} cm^{-1}).

*Fe(III) complex **4-C**:* violet solid (12 mg, yield 30%); IR (ATR): ν_{max} = 1723, 1620 (C=N), 1585, 1529, 1403, 1334, 1233, 1111, 836, 775, 733; HRMS (ESI+): *m/z* calcd for $C_{25}H_{21}FeN_2O_6^+$ $[M]^+$ 486.0509, found 486.0498; UV (HEPES buffer, pH 7.4): λ_{max} = 372 nm.

*Fe(III) complex **5-C**: minor modification brought to general procedure: due to high solubility of this Fe(III)-salen complex in EtOH, the reaction mixture was concentrated under reduced pressure and the resulting solid was washed with Et_2O (x3).* Violet solid (8.7 mg, yield 22%); IR (ATR): ν_{max} = 1715, 1621 (C=N), 1586, 1531, 1406, 1327, 1231, 1140, 1117, 839, 778, 733; HRMS (ESI+): *m/z* calcd for $C_{23}H_{13}F_3FeN_2O_6^+$ $[M]^+$ 526.0070, found 526.0060; UV (HEPES, pH 7.4): λ_{max} = 373 nm.

*Fe(III) complex **6-C**:* violet solid (6.9 mg, yield 18%); IR (ATR): ν_{max} = 1703, 1634 (C=N), 1586, 1401, 1328, 1250, 1162, 1121, 843; HRMS (ESI+): *m/z* calcd for $C_{28}H_{18}FeN_2O_6^+$ $[M]^+$ 534.0509, found 534.0492; UV (HEPES buffer, pH 7.4): λ_{max} = 334 nm.

*Fe(III) complex **7-C***: violet solid (<1.0 mg, yield <5%); IR (ATR): ν_{max} = 1711, 1607 (C=N), 1529, 1404, 1333, 1233, 1156, 841, 733, 703; HRMS (ESI+): m/z calcd for $C_{35}H_{24}FeN_2O_5^+$ $[M]^+$ 610.0822, found 610.0816; UV (HEPES buffer, pH 7.4): λ_{max} = 369 nm.

*Fe(III) complex **8-C***: violet solid (2.6 mg, yield 56%); IR (ATR): ν_{max} = 1727, 1618 (C=N), 1585, 1530, 1470, 1405, 1232, 1111, 840, 777, 731; HRMS (ESI+): *m/z* calcd for $C_{25}H_{20}FeN_2O_6^+$ $[M]^+$ 500.0671, found 500.0665; UV (HEPES buffer, pH 7.4): λ_{max} = 366 nm.

2.4. Fluorescence detection of PPi anion

Experimental details about stock solutions of Fe(III) complexes and analytes

- Stock solutions (10 mM) of Fe(III) complexes were prepared in DMSO (molecular biology grade).
- Stock solutions (10 mM) of anions were prepared in ultrapure water. Unless otherwise stated, sodium salts of anions were used.
- Stock solutions (1.0 mg/mL) of 8-formyl-7-hydroxycoumarin, salen ligands **1-L** and **3-L,** and the corresponding Fe(III) complexes **1-C** and **3-C** used in time-course fluorescence experiments, were prepared in DMSO (UV-spectroscopy grade).
- Stock solution of sodium PPi (NaPPi, 10 mg/mL, 22.4 mM) used in time-course fluorescence experiments, was prepared in ultrapure water using commercial salt NaPPi . 10 H_2O (Prolabo, #28055).

Screening of metal complexes against PPi anion

Small-scale synthesis of metal complexes: stock solutions (10 mM) of metal chloride ($AlCl_3$, $AuCl_3$, $CoCl_2$, $CrCl_3$, $NiCl_2$ and $ZnCl_2$) were prepared in ultrapure water. Salen ligand **1-L** (0.5 mg) was dissolved in EtOH (0.75 mL) and added to the corresponding metal chloride solution (0.25 mL). The resulting reaction mixture was stirred at 50 °C for 2 h then left to stand in 4 °C fridge overnight. The desired metal complex was isolated by centrifugation (8000 rpm, 10 min) and washed with Et_2O (×1). The dried pellets were weighed and stock solutions (10 mM) of these metal complexes were prepared in DMSO.

Screening against PPi anion: see below for procedure described for Fe(III) complexes.

Screening of Fe(III) complexes against PPi anion. Fe(III) complexes **1-C** to **8-C** and PPi were mixed with HEPES buffer (1.6 mL) in a 96-well plate (final concentration of Fe(III) complex: 10 μM). Fluorescence emission at Ex/Em 365/495 nm was recorded after an incubation time of 60 min at 25 °C.

Anion selectivity of Fe(III) complexes for other anions. Fe(III) complexes **1-C** or **3-C** and anions were mixed with HEPES buffer (1.6 mL) in a 96-well plate (final concentration of Fe(III) complex: 10 μM). Fluorescence emission at Ex/Em 495 nm was recorded after an incubation time of 60 min at 25 °C.

Time-course fluorescence experiments and RP-HPLC-fluorescence analyses. All assays were performed at 25 °C (using a temperature control system combined with water circulation) and conducted under continuous mechanical stirring through the use of small stirred blades. Solution of Fe(III) complexes **1-C** and **3-C** (10 μL) was mixed with 2.0 mL of HEPES buffer in 3.5 mL fluorescence quartz cell (final concentration of Fe(III) complex: 10 μM). Fluorescence emission at Ex/Em 365/495 nm (bandwidth = 5 nm, PMT = 600 V) was recorded every 20 s. After 5 min, the appropriate volume of NaPPi solution (corresponding to the number of PPi equiv. to add: 5 to 320 equiv.) was added and the recording of fluorescence signal continued for 2 h. Before and after each kinetic experiment, fluorescence emission spectrum (scan mode) of solution was recorded using the following parameters: Ex at 340 nm (bandwidth = 5 nm), Em within the range 370-650 nm (bandwidth = 5 nm, PMT voltage = 598 V), 1 nm step, full filtering and average time = 0.1 s. *Please note: the availability of a 10 quartz cell rack on SAFAS Flx-Xenius XC spectrofluorimeter enables the measurement of kinetics for multiple samples at the same time.* Blank experiments to assess the stability of 8-formyl-7-hydroxycoumarin, salen ligands **1-L** and **3-L**, and Fe(III) complexes **1-C** and **3-C**, in HEPES buffer were achieved in the same way. Crude solutions from all fluorescence-based assays were directly analyzed by RP-HPLC-fluorescence (injected volume: 20 μL, system A).

Detection limit of Fe(III) complexes 1-C and 3-C for PPi anion. The sensitivity of Fe(III) complexes for PPi was calculated on the basis of the linear relationship between the maximum emission intensity at 495 nm and the concentration of PPi. The intensity at 495 nm increased linearly with the concentration of PPi and a linear measurement is possible until 2 or 4 equiv.

with high accuracy (see Fig. S61 and Fig. S62). The detection limit was calculated with the following equation: detection limit = 3σ/k, where σ is the standard deviation of blank measurement, k is the slope between the fluorescence intensity (F) at 495 nm versus the concentration of NaPPi.

In the case of Fe(III) complex **1-C**, σ was found to be equal to 3.9474 and k = 3.763 ; a LOD of 3.15 μM was found. Linearity from 0-40 μM.

In the case of Fe(III) complex **3-C**, σ was found to be equal to 4.399 and k = 4.702 ; a LOD of 2.81 μM was found. Linearity from 0-19 μM.

3. Results and discussion

3.1 Screening of metal cations

A series of metal cations were screened for their suitability in coumarin-salen derivatives as effective PPi dosimeters. A series of divalent and trivalent metal cations were reacted with coumarin-salen ligand and the resulting complexes isolated following conventional procedures [35]. Fluorescence intensities (λ Ex = 365 nm, λ Em = 495 nm) of metal complexes (10 μM) were measured in HEPES buffer (20 mM, pH = 7.2). The spectral behavior of metal complexes was examined in the absence and presence of PPi (20 equiv., NaPPi as source of pyrophosphate anion) and normalized change in fluorescence intensity was plotted (Fig. 3). An ideal probe achieves a subtle balance between aqueous stability and reactivity toward analyte. Sufficient robustness is required to maintain probe integrity over time to ensure that fluorogenic response is due to the presence of the analyte rather than spontaneous metal leakage and subsequent hydrolysis of the bis-Schiff base bridging ligand. Conversely, if the probe is too robust, insufficient reactivity toward PPi will render the probe unsuitable for its detection purpose. To this end, Fe(III)-salen complex performed the best, showing a 4-fold increase in fluorescence upon addition of PPi (20 equiv.). The paramagnetic nature of Fe(III) has been well-established to readily quench fluorescence of organic-based fluorophores such as coumarins [36-38]. This allows for lower fluorescence background intensities and better signal-to-noise ratios that improve probe sensitivity. Fe(III) cation was thus selected as the preferred metal center for further experimentation.

3.2 Synthesis of coumarin-salen Fe(III) complexes

Coumarin-salen ligands were synthesized from 7-hydroxycoumarin and respective vicinal diamines (a racemic mixture for diamines bearing one or two asymmetric carbon atoms was employed) following literature procedures then complexed with Fe(III) chloride (Scheme 1) [35,39]. 7-Hydroxycoumarin was first subjected to a Duff reaction to install a formyl group at the 8-position with moderate yield (41%). To improve water solubility of this molecule and related bis-Schiff base bridging ligands, attempts were made to introduce ionizable/polar groups (*e.g.*, sulfonic acid/sulfonate SO_3H/SO_3^- or carboxylic acid/carboxylate CO_2H/CO_2^-) within the coumarin scaffold. However, as the Duff reaction proceeds *via* an S_EAr reaction promoted by electron-enriched aromatic substrates, the electron-withdrawing effects of CO_2H or SO_3H were sufficient to deactivate 7-hydroxycoumarin and thus prevented its formylation. Alternative formylation routes *via* the Reimer-Tiemann reaction [40] or Casnati-Skattebøl reaction [41,42] were attempted but led to either irreproducible or unsuccessful results. Consequently, the present study only examined 8-formyl-7-hydroxycoumarin as the fluorescent salicylaldehyde analog possibly released during the disassembly process of Fe(III)-salen complexes. Due to the low pKa value of its phenol (reported in the literature, pKa ca. 6.5) [32], it is quite conceivable that aqueous solubility of this phenol (probably favored by the prevalence of its phenolate form in solution) and related salen ligands at physiological pH is enough to avoid precipitation of fluorescent species during the course of our fluorescence-based assays conducted in HEPES buffer (*vide infra*). Selected racemic vicinal diamines available in their dihydrochloric acid salt form were first converted to their free base form before condensation with 8-formyl-7-hydroxycoumarin to yield the desired salen ligands with isolated yields ranging between 3% and 72%. Unlike other examples, bis-Schiff base derivatives **5-L** and **8-L** were soluble in EtOH and could not be readily purified by precipitation. Instead, preparative thin layer chromatography (Prep TLC) was employed to recover these salen ligands in a pure form. The poor isolated yields (15% and 3% respectively) might be explained by partial decomposition of such bis-imine compounds over silica gel, certainly promoted by the acidic character of this stationary phase. The structure of each coumarin-salen ligand was confirmed by detailed spectroscopic measurements including IR, NMR and ESI-HRMS analyses (see supporting information for the corresponding spectra, Figs. S5-S39).

It should be mentioned, however, that detailed characterization of compound **5-L** derived from 3,3,3-trifluoro-1,2-diaminopropane, was complicated by its poor stability in solution.

Next, complexation with $FeCl_3$ was achieved under conventional conditions and the completion of the reactions was indicated by a rapid color change of mixtures from orange to violet upon addition of this iron salt. Ethanolic solutions containing Fe(III) complexes were subsequently cooled to 4 °C to favor precipitation. Recovery by centrifugation, washes with EtOH and Et_2O and final drying have furnished the targeted metal complexes. These latter compounds were generally insoluble in EtOH except for complex **5-C** which was washed by Et_2O. All Fe(III)-salen complexes were analyzed by ESI-HRMS and IR spectroscopy (see supporting information for results and corresponding spectra, Figs. S40-S57) and subjected to elemental analysis to confirm the nature of the axial ligand (*i.e.*, chloride).

3.3 PPi sensing performances of coumarin-salen Fe(III) complexes

We first focused on the study of the fluorogenic response of compounds **1-C** to **8-C** towards PPi anions under the same conditions. Indeed, in order to find the optimum balance between aqueous stability and fluorogenic reactivity towards this analyte, we considered that systematic structural variations made to salen ligand through the use of different diamine bridges, was an effective way to rapidly identify *ad hoc* probe candidate(s) for practical PPi sensing applications. Therefore, the emission intensity ratio of the test samples (*i.e.*, samples of **1-C** to **8-C** treated with 20 equiv. of NaPPi in HEPES buffer (20 mM, pH 7.2) at 25 °C for 60 min) to the corresponding probe before PPi addition (F/F_0) was systematically determined. From a practical point of view, all measurements were made in 96-well microtiter plates using a fluorescent plate reader, with excitation and emission wavelengths set at 365 and 495 nm, respectively. The results are summarized in Fig. 4. The worst fluorescence responses towards PPi were obtained with Fe(III) complexes **6-C** and **7-C** and may relate to strong steric hindrance on the surrounding environment of metal cation, promoted by the bulky phenyl groups present in the bis-imine backbone. This prevents the PPi-triggered disassembly process from occurring, especially through the flexible mode recently deciphered and proposed by Yadav *et al.* [19]. An unsatisfactory fluorogenic behavior was also observed for complex **4-C** built from a 2,3-diaminobutane-based salen ligand, even if a slightly higher F/F_0 ratio was obtained.

An additional consideration is that the introduction of such sterically bulky groups increases torsional strain barriers against rotation, resulting in metal-ligand complexes poorly reactive toward the targeted anion species. This hypothesis could also be advanced to explain the suboptimal fluorogenic response to PPi observed for Fe(III) complex **8-C** bearing an isopropyl substituent on the diamine backbone, similar to that observed for **4-C**. Most surprising was the fluorescence response observed for complex **5-C** derived from a 1,1,1-trifluoro-2,3-diaminopropane-based salen ligand. Indeed, it was intended that the electron-withdrawing effect of trifluoromethyl group favour partial destabilization of this metal-salen adduct, resulting in a greater fluorogenic reactivity towards PPi, but the opposite behavior was instead observed. On the positive side, activity-based probe **3-C** constructed with 1,2-propylenediamine provided a higher fluorescence response, more than 2.6-fold greater than in the case of sterically hindered compounds previously mentioned, and only slightly less than the prototype probe **1-C** bearing the ethylenediamine bridge. This result is consistent with that obtained by the Zelder group even if the scope of their published study was limited to metal-salen complexes bearing three different diamine bridges derived from ethylenediamine, 1,2-propylenediamine and *ortho*-phenylenediamine respectively [17]. To complete this survey, the effects of diamine bridge length on fluorescence response towards PPi was also assessed. A mediocre fluorescence response, quite similar to that observed with the "bad eggs" **6-C** and **7-C**, was obtained with Fe(III) complex **2-C** based on the 1,3-propylenediamine bridge. The three-carbon linker leads to the formation of a larger and less constrained Fe(III) chelate whose conformation is not necessarily appropriate for linkage isomerism of coordinated PPi anion (*i.e.*, switch from a monodentate to a bidentate coordination mode) that was identified as a crucial step in the PPi-mediated disassembly process of Fe(III)-salen complexes [19]. To conclude, ethylenediamine and 1,2-propylenediamine were identified as the best diamine bridges for the Zelder probe design principle extended to unusual salicylaldehydes such as 8-formyl-7-hydroxycoumarin. Good performances of both Fe(III) complexes **1-C** and **3-C** as PPi-responsive "turn-on" fluorogenic probes were also confirmed by time-course measurements (see Figs. S58 and S59). When **1-C** and **3-C** were mixed with different amounts of NaPPi (5 to 320 equiv.), a moderately rapid and gradual increase of fluorescence emission at 495 nm (λ Ex = 365 nm) was observed and the plateau was reached within 30 min of incubation for assays conducted with a large excess of analyte (80 or more equiv.). Interestingly, fluorescence intensity at this final plateau is close

to the value recorded for the salen ligand solution at the same concentration and roughly divided by 2.5 compared to the solution of 8-formyl-7-hydroxycoumarin knowing that this latter compound is more fluorescent (see section 3.5). These results confirmed the effectiveness of demetallation mediated by PPi anion and that lead to the removal of quenching Fe(III) cation. At this stage of our investigation, there is no conclusive evidence that hydrolysis of bis-Schiff base ligands really occurs to release the fluorescent coumarin derivative. However, since the maximum fluorescence intensity obtained after prolonged incubation, is far lower than the value determined for pure sample of 8-formyl-7-hydroxycoumarin at the same concentration (*i.e.*, 20 μM vs. 10 μM of salen ligands whose complete disassembly leads to 20 μM of 8-formyl-7-hydroxycoumarin), we can argue that in our conditions (HEPES buffer, 20 mM, pH 7.3, 25 °C), this disassembly process does not proceed in a quantitative manner. Blank experiments carried out without NaPPi confirmed aqueous stability of both Fe(III) complexes and 8-formyl-7-hydroxycoumarin with the initial fluorescence signal remaining constant over the duration of assay (more than 2 h). No enhancement of the initial fluorescence intensity of salen ligands was observed even after their prolonged incubation in HEPES buffer; this somewhat surprising result tends to confirm the stability of these bis-Schiff-bases and their limited propensity to release coumarin fluorophore through hydrolysis.

*3.4 Detailed probe performances of coumarin-salen Fe(III) complexes **1-C** and **3-C***

The most promising coumarin-salen Fe(III) complexes **1-C** and **3-C** were brought forward for further characterization as PPi-responsive probes. Selectivity for this anionic analyte over other (poly)phosphate species including inorganic phosphate (Pi), ADP and ATP, was assessed through fluorescence titration experiments (Fig. 5). Pi did not produce discernible changes in fluorescence emission intensity ($F/F_0 = 1$), confirming its inability to demetallate **1-C** and **3-C**. This positive result is in agreement with observations made by the Zelder group and is typical of the disassembly strategy applied to fluorogenic metal-salen based probes [15-17]. Conversely, a poor selectivity of **1-C** for PPi over ADP and ATP was demonstrated. Indeed, the values of the emission intensity ratio are in the same order of magnitude: 4.1 for ADP, 5.2 for ATP and 7.1 for PPi. A more encouraging result was obtained with 1,2-propylenediamine-

based Fe(III) complex **3-C** that showed a stronger preference for PPi as revealed by the collected F/F_0 values: 3.2 for ADP, 4.5 for ATP and 9.2 for PPi. This behavior is again quite consistent with results obtained by the Zelder group with "flexible" Fe(III)-salen complex **9**, and interpreted through an unusual binding isomerism mechanism of PPi anion. It should also be noted that, when the assay buffer was changed to Tris.HCl (20 mM, pH 9.0), a drastic and positive change in selectivity occurred even if fluorescence background is higher. Only the addition of PPi analyte elicited a prominent fluorescence enhancement of both complexes **1-C** and **3-C** (Fig. 6).

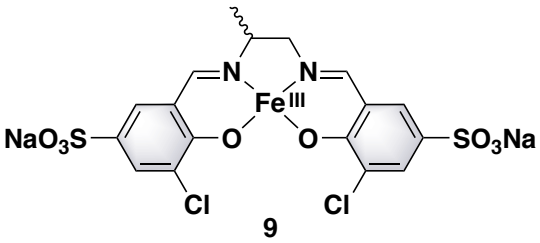

9

This finding may be particularly useful for the implementation of fluorogenic metal-salen complexes in sensing applications aimed at evaluating PPi content in complex matrices containing multiple phosphate species, through the choice of the most suited buffer for sample formulation. Not surprisingly, titration experiments carried out with other frequently encountered anions (NO_2^-, F^-, SCN^-, $CH_3CO_2^-$, HCO_3^-, CO_3^{2-}, Cl^-, Br^-, and SO_4^{2-}) did not reveal changes in low background fluorescence of both complexes **1-C** and **3-C**, thus further supporting selectivity of Fe(III)-salen complexes for polyphosphates (Fig. 7 and Fig. S60). In terms of graduated fluorogenic response, dose responses up to 4 equiv. of PPi for complex **1-C** (R^2 = 0.96) and up to 2 equiv. of PPi for complex **3-C** (R^2 = 0.96) were observed (see the Supporting Information, Fig. S61 and S62). This suggests that the slight stability improvement afforded by the 1,2-propylenediamine bridge alters metal-ligand dissociation sufficiently to extend the range of PPi detection beyond the original stoichiometry. The limits of detection (LOD) for complexes **1-C** and **3-C** were found to be 3.15 μM and 2.81 μM respectively. These values are comparable to that reported for Fe(III)-salen complex **9** (LOD 1.50 μM). The probe performances detailed above confirm that the reporter 8-formyl-7-hydroxycoumarin is fully compatible with the PPi-responsive probe design principle based on a disassembly

mechanism. However, its modest fluorescence properties in physiological buffers (see section 3.5) are not able to achieve impressive outcomes for PPi fluorogenic sensing.

*3.5 Photophysical properties of 8-formyl-7-hydroxycoumarin, coumarin-salen ligands **1-L** and **3-L** and related Fe(III) complexes **1-C** and **3-C***

In order to correlate the PPi sensing performances of **1-C** and **3-C** with their spectral properties, a comprehensive photophysical study of compounds based on ethylene- and 1,2-propylenediamine backbones (both ligands and Fe(III) complexes) was carried out. Spectral properties of **1-L**, **3-L**, **1-C** and **3-C** were investigated through the recording of their absorption and fluorescence spectra in HEPES aqueous solution (20 mM, pH 7.3), a common buffer for biological sciences particularly well suited for fluorescence-based assays involving polyphosphate species and considered in this study (*vide supra*). Photophysical characterization of 8-formyl-7-hydroxycoumarin was also conducted under the same conditions in order to provide a reliable benchmark of comparison. Collected data are gathered in Table 1 and overlays of the normalized absorption/excitation/emission spectra in HEPES buffer are displayed in Fig. 8 (see Figs. S2 and S63 for the absorption/fluorescence spectra of 8-formyl-7-hydroxycoumarin and salicylaldehyde respectively). UV-visible absorption spectra of both salen ligands are characterized by two maxima at ca. 280 and 350 nm and a pronounced shoulder centered at ca. 400 nm. The most intense absorption band centered at ca. 350 nm is assigned to S0-S1 transition for the neutral form of salen ligand (electronic transition of π-π^* type for bis-phenol form) whereas the long-wavelength shoulder may be interpreted as the spectral signature of mono- and/or bis-anions which are minor species in aq. buffer at pH 7.3 (mono- and/or bis-phenolate forms). Indeed, it is well known that deprotonation of 7-hydroxycoumarin raises the HOMO level more than the LUMO level leading to an energy gap decrease between these two frontier molecular orbitals involved in the π-π^* electronic transition [43]. Moreover, minor contribution of n-π^* electronic transition of nitrogen lone pair of imine moieties, to this intense shoulder cannot be totally ruled out even though its molar extinction coefficient is very low as already observed, for instance, by Zelder and co-workers for salen ligands based on more conventional salicylaldehydes [17]. The UV-vis absorption curve profile of the corresponding Fe(III) complexes is dramatically different

with a broad and unstructured band centered at 355-360 nm but mostly, a continuous increase in extinction from long to shorter wavelengths that prevents the visualization of expected ligand-to-metal charge transfer (LMCT) band. This spectral behavior is typical of Rayleigh-Tyndall scattering and is promoted by aggregates or colloidal suspensions in aqueous solution. In the present case, the lack of water-solubilizing group(s) onto the coumarin scaffold undoubtedly contributes to aggregate formation in HEPES buffer. For the determination of fluorescence parameters of both salen ligands and Fe(III) complexes, 340 nm was chosen as excitation wavelength to ensure that entire emission spectra will be recovered even if it does not correspond to the excitation maximum of the most emissive species (see the corresponding excitation spectra of salen ligands **1-L** and **3-L**). As expected, and illustrated in Fig. 8, salen ligands derived from 8-formyl-7-hydroxycoumarin exhibit a broad and less structured emission band within the blue-cyan spectral range, centered at 510 nm and 477 nm respectively (full-width at half maximum (FWHM) $\Delta\lambda_{1/2max}$ in the range 90-130 nm) and red-shifted compared to this parent phenol-based fluorophore (bathochromic shift of ca. 40 nm and 10 nm respectively). Using 7-hydroxycoumarin in phosphate buffer (PB, 100 mM, pH 7.4) as reference (Φ_F = 76%), we have determined the relative fluorescence quantum yield of each compound in HEPES buffer. The low values obtained for 8-formyl-7-hydroxycoumarin (Φ_F = 4%) and the two salen ligands **1-L** and **3-L** (Φ_F = 1% and 2%) are not surprising and interpreted for salicylaldehyde derivatives as a possible charge transfer from the coumarin HOMO to the aldehyde carbonyl LUMO [44]. The same hypothesis could be advanced for 7-hydroxycoumarins bearing an imine moiety as with salen ligands **1-L** and **3-L**, even if other photophysical mechanisms promoted by the close spatial proximity between fluorophore units (*e.g.*, self-quenching (homo-FRET) and H-type dimer formation) could also contribute to the modest fluorescence efficiency of these diamine bridged bis-coumarin derivatives. Interestingly, the lack of a perfect overlap between absorption and excitation spectra has confirmed that deprotonation of phenol moieties occurs in the excited state [43]. At pH 7.3, phenolate forms are not the prevailing species and marked differences in the absorbance maxima of neutral and anion forms are thus observed: 65 nm for 8-formyl-7-hydroxycoumarin, 47 nm for **1-L** and 75 nm for **3-L**. Over the course of these spectral measurements, we have also highlighted an unexpected and interesting behavior of salen ligand based on 1,2-propylenediamine (**3-L**). After storage of its stock solution (prepared in DMSO) for several days followed by a fast defrosting with a water-bath at 40 °C, partial and

irreversible precipitation of ligand was observed. The repeat recording of absorption and fluorescence spectra of the supernatant, showed clearly the presence of a novel form in solution, characterized by a red-shifted (23 nm) maximum emission wavelength and the halving of fluorescence quantum yield (see Figs. S20, S21 and S64). At this stage, an explanation for this remains elusive despite the possibility of an equilibrium between geometrical isomers (*i.e.*, E-Z isomerism of imines) cannot be fully excluded. The last predictable information gained through this photophysical study is the ability of ferric cations to readily quench blue-cyan fluorescence of salen ligands **1-L** and **3-L**. We managed to record fluorescence excitation/emission spectra of Fe(III) complexes **1-C** and **3-C** but only using high concentrated solutions (ca. 20 μM). Under these abnormal conditions, it was not possible to apply standard methodology for determining the corresponding very low fluorescence quantum yields. Therefore, both complexes were assumed to be non-fluorescent.

*3.6 Mechanistic study of the PPi-mediated disassembly process of coumarin-salen Fe(III) complexes **1-C** and **3-C***

In order to confirm that the blue-cyan fluorescence detected during the endpoint and time-course measurements (see section 3.3) was due to the release of 8-formyl-7-hydroxycoumarin, some reaction mixtures arising from kinetics experiments were subjected to RP-HPLC-fluorescence analyses (see Fig. 9 for selected RP-HPLC elution profiles related to fluorogenic activation of **1-C** and Figs. S65-S86). Since aqueous acidic conditions (*e.g.*, 0.1% formic acid) typically used in RP-HPLC eluents are not compatible with the stability of salen ligands (*i.e.*, hydrolysis of their imine linkages) and unsuited for detecting fluorescence emission of phenol-based fluorophores such as 7-hydroxycoumarins, aqueous triethylammonium acetate (TEAA, 25 mM, pH 7.0) and MeCN without additive were used as mobile phase. As expected, the elution profiles of reaction mixtures between coumarin-salen Fe(III) complex (**1C** or **3C**) and excess of PPi anion revealed a peak (t_R = 2.5-2.6 min) corresponding to salen ligand (**1-L** or **3-L**), confirmed by comparison with authentic samples of these bis-Schiff bases as references. The observed abnormal peak shape (*i.e.*, split and broad) may be interpreted as follows: (1) a mixture of geometrical isomers (E-Z isomerism of imines in the case of ethylenediamine bridge) and/or diastereomers (E-Z isomerism of imines

and racemic mixture of 1,2-propylenediamine used as bridge) for the released salen ligand, (2) mixture of compounds arising from partial hydrolysis of salen ligand into 8-formyl-7-hydroxycoumarin during assays and/or RP-HPLC analyses, and/or (3) several protonation states at pH 7.0 for salen ligands and 8-formyl-7-hydroxycoumarin. Control experiments (*i.e.*, prolonged incubation of Fe(III) complexes in HEPES buffer) confirmed the full stability of metal-based PPi-responsive probes at pH 7.3 since the split and broad peak at t_R = 2.5-2.6 min typical of fluorescent demetalated species, but of a very low intensity, was observed on the detection channel Ex/Em 365/495 nm (Fig. 9 and Fig. S77). Partial hydrolysis of both salen ligands into 8-formyl-7-hydroxycoumarin appeared to occur as revealed by further control experiments involving prolonged incubation of **1-L** and **3-L** in HEPES buffer with or without a large excess of PPi anion (80 equiv.) (Figs. S75 and S86). Indeed, we noted a change in the peak shape with a modest real retention time shift from 2.6 min (mainly assigned to salen ligand) to 2.5 min (mainly assigned to 8-formyl-7-hydroxycoumarin). However, this disassembly process based on the hydrolysis of imine linkages is far from being quantitative in our conditions (2 h of incubation at 25 °C, in HEPES buffer, pH 7.3). Typically, our well-established analytical methodology routinely used for validating reaction-based fluorescent probes also involves RP-HPLC-MS analyses [45]. Indeed, this may provide further evidence for the claimed detection mechanism and allows estimation of the conversion rate of the fluorogenic disassembly process occurring in HEPES buffer. However, the use of aqueous TEAA as mobile phase made ESI-MS analyses complicated (difficulties to ionize compounds despite the screening of different sets of parameters (*e.g.*, probe temperature, needle and cone voltages), and the presence of a large amount of PPi anion in reaction mixtures negatively impacted retention behavior of compounds to be detected and quantified. Consequently, no conclusive results have been obtained and we have thus completed our mechanistic study with some ^{1}H NMR experiments conducted in a mixture of D_2O and DMSO-d_6 (9 : 1, v/v) (see Supporting Information, Figs. S87 and S88). Addition of PPi (10 equiv.) to a solution of Fe(III) complex **3-C** (2 mM) led to the occurrence of a set of signals (aldehyde and aromatic protons) unambiguously assigned to 8-formyl-7-hydroxycoumarin, within 60 min (Fig. S87). Under these unbuffered conditions, we did not observe any signals from the salen ligand **3-L**, thus suggesting its rapid and quantitative hydrolysis into the corresponding fluorescent salicylaldehyde and 1,2-propylenediamine once the metal cation was displaced. The recording of further ^{31}P NMR spectra revealed the same spectral behavior reported by the Zelder group

[17] (*i.e.*, an upfield shift of 1.67 ppm along with a broadening of the singlet at -8.68 ppm), confirming the interaction between Fe(III) cation and PPi anion and final formation of $Fe(PPi)_n$ species through metal displacement reaction (Fig. S88). There is an apparent contradiction between results arising from RP-HPLC-fluorescence analyses on the one hand and NMR measurements on the other hand. In the first case, we detected a mixture of salen ligand and 8-formyl-7-hydroxycoumarin whereas this latter salicylaldehyde was only observed on ^1H NMR spectra. We can conclude that the hydrolysis of bis-Schiff bases is strongly influenced by the composition and pH of aqueous media in which Fe(III)-salen complexes are used. Since the fluorescence quantum yield of 8-formyl-7-hydroxycoumarin is twice to four times higher than that of salen ligands **1-L** and **3-L**, the choice of an aqueous buffer promoting imine hydrolysis should be preferred when a maximum detection sensitivity is sought.

4. Conclusion

In this study, we have revisited the fluorogenic disassembly approach recently proposed by the Zelder group to achieve selective and sensitive detection of PPi anion in various matrices. Our methodology based on both screening of eight different vicinal diamines as the bridging ligand and the use of 8-formyl-7-hydroxycoumarin as the fluorescent salicylaldehyde enabled the preparation of a set of novel coumarin-salen Fe(III) complexes acting as PPi-responsive "turn-on" fluorogenic probes. A robust and easily implementable analytical methodology mainly based on fluorescence assays has been applied to rapidly assess sensing performances of these metal-based fluorescent probes. We have highlighted that most structural alterations to the parent ethylenediamine-based bis-imine bridge resulted in decreased fluorogenic responses towards PPi. This has been mainly attributed to stability enhancement of the Fe(III)-salen complex, resulting to a lower ability to undergo metal displacement. These findings are consistent with results obtained by the Zelder group despite significant differences in the structure of fluorescent salicylaldehyde. Thus, coumarin-salen Fe(III) complexes **1-C** and **3-C** derived from ethylenediamine and racemic 1,2-propylenediamine backbones respectively have yielded the best PPi-sensing performances. Furthermore, coumarin-salen Fe(III) complexes **1-C** and **3-C** displayed exquisite selectivity for PPi anions over related phosphate ions in Tris.HCl solutions. However, the use of 8-formyl-7-hydroxycoumarin as fluorescent

reporter did not enable to reach LOD values dramatically lower than those obtained with more conventional salicylaldehyde derivatives. A further extension of the present methodology to phenol-based fluorophores whose *ortho*-formylation leads to a significant increase of their fluorescence quantum yield, is required and currently under investigation in our both labs. Aside from these photophysical considerations, there is also a genuine need to optimize water solubility of such fluorescent salicylaldehydes, to enhance both their resistance to aggregation in aq. media and overall hydrophilicity of the related metal-salen complexes. In light of these requirements, *ortho*-salicylaldehydes based on 4-hydroxy-1,8-naphthalimide scaffold may be particularly well suited for achieving high-performance fluorogenic metal-salen based probes [46-48],[49]. Our study also illustrated the interest to implement both fluorescence time-course measurements and RP-HPLC-fluorescence analyses for the accurate characterization of PPi-mediated disassembly mechanism of Fe(III)-salen complexes. This analytical methodology is therefore complementary to mechanistic studies reported by the Zelder group and should be helpful for improving sensing performances of next-generation fluorogenic metal-salen complexes intended for applications in both bioanalysis of nucleic acids and biocatalyzed oligonucleotide synthesis. Lastly, the wider availability of metal-salen complexes derived from visible light dyes (*i.e.*, *ortho*-formyl derivatives of 7-hydroxycoumarins [44], 4-hydroxy-1,8-naphthalimides[49], fluoresceins [42,50-52], rhodols [53], ...), capable of acting as efficient photosensitizers, should be of great interest to organic chemists working in the field of photoredox catalysis [54].

Author contributions

Eunice Y.-L. Hui: Conceptualization, Investigation, Formal analysis. **Dillon W. P. Tay:** Conceptualization, Investigation, Formal analysis, Writing - original draft. **Jean-Alexandre Richard:** Initial conceptualization, Funding acquisition, Early investigation, Writing - review. **Zuzana Pohancenikova:** Investigation. **Kévin Renault:** Conceptualization, Investigation, Formal analysis, Writing - review. **Anthony Romieu:** Conceptualization, Investigation, Formal analysis, Writing - original draft, Writing - review & editing, Funding acquisition. **Lim Yee Hwee:** Conceptualization, Investigation, Formal analysis, Writing - review & editing, Funding acquisition.

Declaration of competing interest

The authors declare that they have no known competing financial interests or personal relationships that could have appeared to influence the work reported in this paper.

Acknowledgements

This work was supported by the Agency for Science, Technology & Research (A*STAR), Institute of Sustainability for Chemicals, Energy and Environment (ISCE^2), and the Singapore National Research Foundation - Agence Nationale de la Recherche (NRF-ANR) Grant (no. NRF2018-NRF-ANR035). For the french partner, this is also part of the project "MULTIMOD", supported by the Conseil Régional de Bourgogne Franche-Comté and the European Union through the PO FEDER-FSE Bourgogne 2014/2020 programs. Financial support from the Agence Nationale de la Recherche (ANR, AAPG 2018, PRCI, LuminoManufacOligo, ANR-18-CE07-0045), especially for the funding of a postdoc fellowship (Dr. Kévin Renault) and a young engineer position (Miss Zuzana Pohancenikova, chemistry engineer ENSCM) is also greatly acknowledged. The authors from ISCE^2 (A*STAR, Singapore) thank Dr. Choon Boon Cheong (ISCE^2) for his help in some NMR analyses and characterizations. The authors from ICMUB (Dijon, France) thank the "Plateforme d'Analyse Chimique et de Synthèse Moléculaire de l'Université de Bourgogne" (PACSMUB, http://www.wpcm.fr) for access to analytical and molecular spectroscopy instruments. These authors also thank Miss Marie-José Penouilh (University of Burgundy, PACSMUB) and Dr. Quentin Bonnin (CNRS, PACSMUB) for their assistance during RP-HPLC-MS analyses, Prof. Ewen Bodio (University of Burgundy, ICMUB, UMR CNRS 6302, OCS team) for access to SAFAS Flx-Xenius XC spectrofluorimeter, Dr. Valentin Quesneau (UBFC, ICMUB, 2019-2021) for purification of salicylaldehyde used as reference in the photophysical studies, and Prof. Dr. Felix H. Zelder (University of Zurich, Department of Chemistry, Zurich, Switzerland) for fruitful discussions regarding purification and mass characterization of Fe(III)-salen complexes.

Supplementary data

Supplementary data (52 pages) to this article can be found online at https://doi.org/10.1016/j.dyepig.2022.110708.

References and note

A preprint was previously posted on ChemRxiv, see: 10.26434/chemrxiv-2022-xqlqc

[1] Achbergerová L, Nahálka J. Polyphosphate - an ancient energy source and active metabolic regulator. Microb. Cell Fact. 2011;10:63. https://doi.org/10.1186/1475-2859-10-63

[2] Hunter T, Sefton BM. Protein phosphorylation parts A and B. San Diego: Academic Press; 1991.

[3] Cowart RE, Swope S, Loh TT, Chasteen ND, Bates GW. The exchange of Fe^{3+} between pyrophosphate and transferrin. Probing the nature of an intermediate complex with stopped flow kinetics, rapid multimixing, and electron paramagnetic resonance spectroscopy. J. Biol. Chem. 1986;261:4607-14. https://doi.org/https://doi.org/10.1016/S0021-9258(17)38545-9

[4] Xu S-Q, He M, Yu H-P, Wang X-Y, Tan X-L, Lu B, Sun X, Zhou Y-K, Yao Q-F, Xu Y-J, Zhang Z-R. Bioluminescent Method for Detecting Telomerase Activity. Clin. Chem. 2002;48:1016-20. https://doi.org/10.1093/clinchem/48.7.1016

[5] Burton A, Hu X, Saiardi A. Are inositol pyrophosphates signalling molecules? J. Cell Physiol. 2009;220:8-15. https://doi.org/https://doi.org/10.1002/jcp.21763

[6] Kottur J, Nair DT. Pyrophosphate hydrolysis is an intrinsic and critical step of the DNA synthesis reaction. Nucleic Acids Res. 2018;46:5875-85. https://doi.org/10.1093/nar/gky402

[7] Roberts TC, Langer R, Wood MJA. Advances in oligonucleotide drug delivery. Nat. Rev. Drug Discov. 2020;19:673-94. https://doi.org/10.1038/s41573-020-0075-7

[8] Davies IW, Welch CJ. Looking Forward in Pharmaceutical Process Chemistry. Science 2009;325:701-04. https://doi.org/doi:10.1126/science.1174501

[9] Jensen MA, Davis RW. Template-Independent Enzymatic Oligonucleotide Synthesis (TiEOS): Its History, Prospects, and Challenges. Biochemistry 2018;57:1821-32. https://doi.org/10.1021/acs.biochem.7b00937

[10] Lee S, Yuen KKY, Jolliffe KA, Yoon J. Fluorescent and colorimetric chemosensors for pyrophosphate. Chem. Soc. Rev. 2015;44:1749-62. https://doi.org/10.1039/c4cs00353e

[11] Xu Z, Choi JY, Yoon J. Fluorescence Sensing of Dihydrogen Phosphate and Pyrophosphate using Imidazolium Anthracene Derivatives. Bull. Korean Chem. Soc. 2011;32:1371-74. https://doi.org/10.5012/bkcs.2011.32.4.1371

[12] Ngo HT, Liu X, Jolliffe KA. Anion recognition and sensing with Zn(II)–dipicolylamine complexes. Chem. Soc. Rev. 2012;41:4928-65. https://doi.org/10.1039/c2cs35087d

[13] Anbu S, Paul A, Stasiuk GJ, Pombeiro AJL. Recent developments in molecular sensor designs for inorganic pyrophosphate detection and biological imaging. Coord. Chem. Rev. 2021;431:213744. https://doi.org/https://doi.org/10.1016/j.ccr.2020.213744

[14] Wongkongkatep J, Ojida A, Hamachi I. Fluorescence Sensing of Inorganic Phosphate and Pyrophosphate Using Small Molecular Sensors and Their Applications. Top. Curr. Chem. 2017;375:30. https://doi.org/10.1007/s41061-017-0120-0

[15] Kumari N, Zelder F. Detecting biologically relevant phosphates with locked salicylaldehyde probes in water. Chem. Commun. 2015;51:17170-73. https://doi.org/10.1039/c5cc07413d

[16] Kumari N, Huang H, Chao H, Gasser G, Zelder F. A Disassembly Strategy for Imaging Endogenous Pyrophosphate in Mitochondria by Using an Fe^{III}–salen Complex. ChemBioChem 2016;17:1211-15. https://doi.org/https://doi.org/10.1002/cbic.201600195

[17] Yadav P, Jakubaszek M, Spingler B, Goud B, Gasser G, Zelder F. Fe^{III}–Salen-Based Probes for the Selective and Sensitive Detection of E450 in Foodstuff. Chem. - Eur. J. 2020;26:5717-23. https://doi.org/https://doi.org/10.1002/chem.201905686

[18] Yadav P, Zelder F. Metal-Salen-based Probes for the Selective Detection of Phosphates via a Disassembly Approach. Chimia 2020;74:252-56. https://doi.org/10.2533/chimia.2020.252

[19] Yadav P, Blacque O, Roodt A, Zelder F. Induced fit activity-based sensing: a mechanistic study of pyrophosphate detection with a "flexible" Fe-salen complex. Inorg. Chem. Front. 2021;8:4313-23. https://doi.org/10.1039/d1qi00209k

[20] Winkler D, Banke S, Kurz P. Fluorimetric Detection of Phosphates in Water Using a Disassembly Approach: A Comparison of Fe^{III}-, Zn^{II}-, Mn^{II}- and Mn^{III}-salen Complexes. Z. Anorg. Allg. Chem. 2020;646:933-39. https://doi.org/https://doi.org/10.1002/zaac.202000045

[21] Jung HS, Han JH, Kim ZH, Kang C, Kim JS. Coumarin-Cu(II) Ensemble-Based Cyanide Sensing Chemodosimeter. Org. Lett. 2011;13:5056-59. https://doi.org/10.1021/ol2018856

[22] Liu J, Cheng J, Ma X, Zhou X, Xiang H. Photophysical properties and pH sensing applications of luminescent salicylaldehyde derivatives. Res. Chem. Intermed. 2016;42:5027-48. https://doi.org/10.1007/s11164-015-2343-4

[23] Cao D, Liu Z, Verwilst P, Koo S, Jangjili P, Kim JS, Lin W. Coumarin-Based Small-Molecule Fluorescent Chemosensors. Chem. Rev. 2019;119:10403-519. https://doi.org/10.1021/acs.chemrev.9b00145

[24] Kulkarni A, Patil SA, Badami PS. Synthesis, characterization, DNA cleavage and in vitro antimicrobial studies of La(III), Th(IV) and VO(IV) complexes with Schiff bases of coumarin derivatives. Eur. J. Med. Chem. 2009;44:2904-12. https://doi.org/10.1016/j.ejmech.2008.12.012

[25] Kulkarni A, Patil SA, Badami PS. DNA cleavage and in vitro antimicrobial studies of Co(II), Ni(II), and Cu(II) complexes with ONNO donor Schiff bases: Synthesis, spectral characterization, and electrochemical studies. J. Enzyme Inhib. Med. Chem. 2010;25:87-96. https://doi.org/10.3109/14756360903017791

[26] Sharma V, Arora EK, Cardoza S. Synthesis, antioxidant, antibacterial, and DFT study on a coumarin based salen-type Schiff base and its copper complex. Chem. Pap. 2016;70:1493-502. https://doi.org/10.1515/chempap-2016-0083

[27] Gillard M, Weynand J, Bonnet H, Loiseau F, Decottignies A, Dejeu J, Defrancq E, Elias B. Flexible RuII Schiff Base Complexes: G-Quadruplex DNA Binding and Photo-Induced Cancer Cell Death. Chem. - Eur. J. 2020;26:13849-60. https://doi.org/10.1002/chem.202001409

[28] Mestizo PD, Narvaez DM, Pinzon-Ulloa JA, Di Bello DT, Franco-Ulloa S, Macias MA, Groot H, Miscione GP, Suescun L, Hurtado JJ. Novel complexes with ONNO tetradentate coumarin schiff-base donor ligands: x-ray structures, DFT calculations, molecular dynamics and potential anticarcinogenic activity. Biometals 2021;34:119-40. https://doi.org/10.1007/s10534-020-00268-8

[29] Nunez-Dallos N, Posada AF, Hurtado J. Coumarin salen-based zinc complex for solvent-free ring opening polymerization of ε-caprolactone. Tetrahedron Lett. 2017;58:977-80. https://doi.org/10.1016/j.tetlet.2017.01.088

[30] Fulmer GR, Miller AJM, Sherden NH, Gottlieb HE, Nudelman A, Stoltz BM, Bercaw JE, Goldberg KI. NMR Chemical Shifts of Trace Impurities: Common Laboratory Solvents, Organics, and Gases in Deuterated Solvents Relevant to the Organometallic Chemist. Organometallics 2010;29:2176-79. https://doi.org/10.1021/om100106e

[31] Setsukinai K-i, Urano Y, Kikuchi K, Higuchi T, Nagano T. Fluorescence switching by O-dearylation of 7-aryloxycoumarins. Development of novel fluorescence probes to detect reactive oxygen species with high selectivity. J. Chem. Soc., Perkin Trans. 2 2000:2453-57. https://doi.org/10.1039/B006449L

[32] Skarga VV, Negrebetsky VV, Baukov YI, Malakhov MV. Twice as Nice: The Duff Formylation of Umbelliferone Revised. Molecules 2021;26. https://doi.org/10.3390/molecules26247482

[33] Yuan J, Li L, Shen Y, Zeng X, Mou L. Fluorescent probe-based method for monitoring Zn^{2+} in cancer cells, (China), CN104498579A.

[34] Shen Y, Zhao Y, Zeng X, Mou L. Method for detecting trace magnesium ions, zinc ions, and fluoride ions by ratio absorption ultraviolet spectrometry, (China), CN104266989B.

[35] Salanti A, Orlandi M, Tolppa E-L, Zoia L. Oxidation of Isoeugenol by Salen Complexes with Bulky Substituents. Int. J. Mol. Sci. 2010;11:912-26.

[36] Wei T-B, Zhang P, Shi B-B, Chen P, Lin Q, Liu J, Zhang Y-M. A highly selective chemosensor for colorimetric detection of Fe^{3+} and fluorescence turn-on response of Zn^{2+}. Dyes Pigm. 2013;97:297-302. https://doi.org/https://doi.org/10.1016/j.dyepig.2012.12.025

[37] Wang W, Wu J, Liu Q, Gao Y, Liu H, Zhao B. A highly selective coumarin-based chemosensor for the sequential detection of Fe^{3+} and pyrophosphate and its application in living cell imaging. Tetrahedron Lett. 2018;59:1860-65. https://doi.org/https://doi.org/10.1016/j.tetlet.2018.04.007

[38] Sahoo SK, Crisponi G. Recent Advances on Iron(III) Selective Fluorescent Probes with Possible Applications in Bioimaging. Molecules 2019;24:3267. https://doi.org/10.3390/molecules24183267

[39] Lindoy LF, Meehan GV, Svenstrup N. Mono- and Diformylation of 4-Substituted Phenols: A New Application of the Duff Reaction. Synthesis 1998;1998:1029-32.

[40] Liu W, Xu L, Sheng R, Wang P, Li H, Wu S. A Water-Soluble "Switching On" Fluorescent Chemosensor of Selectivity to Cd^{2+}. Org. Lett. 2007;9:3829-32. https://doi.org/10.1021/ol701620h

[41] Casiraghi G, Casnati G, Puglia G, Sartori G, Terenghi G. Selective reactions between phenols and formaldehyde. A novel route to salicylaldehydes. J. Chem. Soc., Perkin Trans. 1 1980:1862-65. https://doi.org/10.1039/p19800001862

[42] Wang W, Rusin O, Xu X, Kim KK, Escobedo JO, Fakayode SO, Fletcher KA, Lowry M, Schowalter CM, Lawrence CM, Fronczek FR, Warner IM, Strongin RM. Detection of

Homocysteine and Cysteine. J. Am. Chem. Soc. 2005;127:15949-58. https://doi.org/10.1021/ja054962n
[43] Hurley JJM, Meisner QJ, Huang C, Zhu L. Hydroxyaromatic Fluorophores. ACS Omega 2021;6:3447-62. https://doi.org/10.1021/acsomega.0c04611
[44] Lee K-S, Kim T-K, Lee JH, Kim H-J, Hong J-I. Fluorescence turn-on probe for homocysteine and cysteine in water. Chem. Commun. 2008:6173-75. https://doi.org/10.1039/B814581D
[45] Jenni S, Renault K, Dejouy G, Debieu S, Laly M, Romieu A. In Situ Synthesis of Phenoxazine Dyes in Water: Application for "Turn-On" Fluorogenic and Chromogenic Detection of Nitric Oxide. ChemPhotoChem 2022;6:e202100268. https://doi.org/https://doi.org/10.1002/cptc.202100268
[46] Dong H-Q, Wei T-B, Ma X-Q, Yang Q-Y, Zhang Y-F, Sun Y-J, Shi B-B, Yao H, Zhang Y-M, Lin Q. 1,8-Naphthalimide-based fluorescent chemosensors: recent advances and perspectives. J. Mater. Chem. C 2020;8:13501-29. https://doi.org/10.1039/D0TC03681A
[47] Zhu H, Liu C, Su M, Rong X, Zhang Y, Wang X, Wang K, Li X, Yu Y, Zhang X, Zhu B. Recent advances in 4-hydroxy-1,8-naphthalimide-based small-molecule fluorescent probes. Coord. Chem. Rev. 2021;448:214153. https://doi.org/https://doi.org/10.1016/j.ccr.2021.214153
[48] Gopala L, Cha Y, Lee MH. Versatile naphthalimides: Their optical and biological behavior and applications from sensing to therapeutic purposes. Dyes Pigm. 2022;201:110195. https://doi.org/https://doi.org/10.1016/j.dyepig.2022.110195
[49] Wang R, Ding J, Zhang Y. Naphthalimide/benzimide-based excited-state intramolecular proton transfer active luminogens: aggregation-induced enhanced emission and potential for chemical modification. New J. Chem. 2019;43:9152-61. https://doi.org/10.1039/C9NJ01685F
[50] Burdette SC, Walkup GK, Spingler B, Tsien RY, Lippard SJ. Fluorescent Sensors for Zn2+ Based on a Fluorescein Platform: Synthesis, Properties and Intracellular Distribution. J. Am. Chem. Soc. 2001;123:7831-41. https://doi.org/10.1021/ja010059l
[51] Barve A, Lowry M, Escobedo JO, Thainashmuthu J, Strongin RM. Fluorescein Tri-Aldehyde Promotes the Selective Detection of Homocysteine. J. Fluoresc. 2016;26:731-37. https://doi.org/10.1007/s10895-015-1762-3
[52] Ali A, Kamra M, Roy S, Muniyappa K, Bhattacharya S. Enhanced G-Quadruplex DNA Stabilization and Telomerase Inhibition by Novel Fluorescein Derived Salen and Salphen Based Ni(II) and Pd(II) Complexes. Bioconjugate Chem. 2017;28:341-52. https://doi.org/10.1021/acs.bioconjchem.6b00433
[53] Zhang Y, Ma L, Tang C, Pan S, Shi D, Wang S, Li M, Guo Y. A highly sensitive and rapidly responding fluorescent probe based on a rhodol fluorophore for imaging endogenous hypochlorite in living mice. J. Mater. Chem. B 2018;6:725-31. https://doi.org/10.1039/C7TB02862H
[54] Gualandi A, Marchini M, Mengozzi L, Kidanu HT, Franc A, Ceroni P, Cozzi PG. Aluminum(III) Salen Complexes as Active Photoredox Catalysts. Eur. J. Org. Chem. 2020:1486-90. https://doi.org/https://doi.org/10.1002/ejoc.201901086

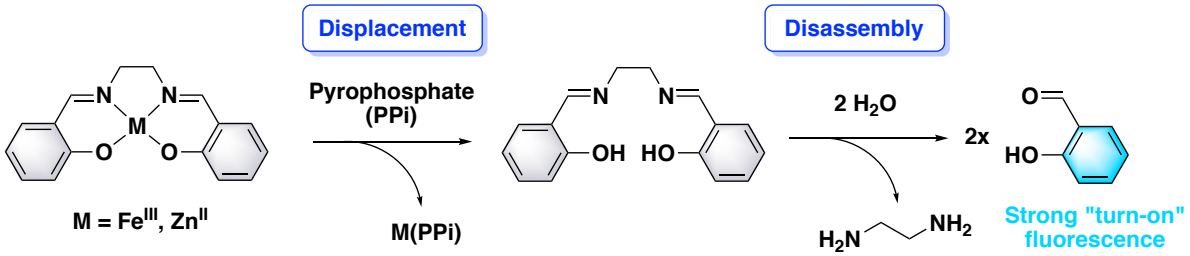

Fig. 1. Overview of the disassembly approach proposed by the Zelder group for "turn-on" fluorogenic detection of PPi anion through the release of salicylaldehyde. *Please note: for clarity, axial ligand (H_2O or Cl^-) on metal-salen complexes is omitted.*

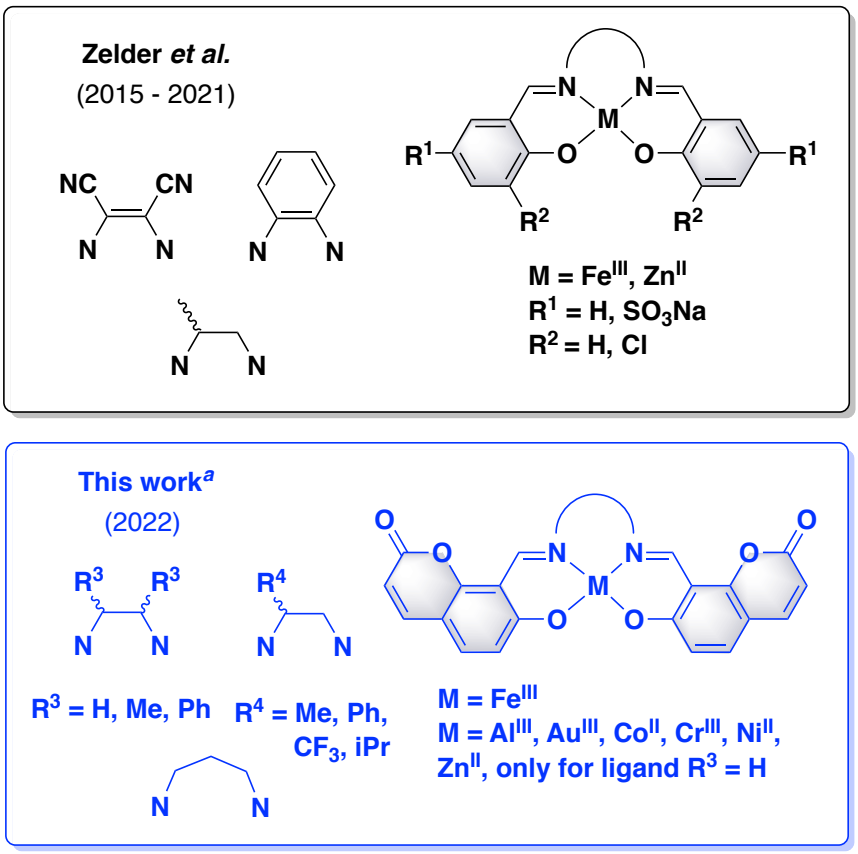

Fig. 2. (top) Previous works from the Zelder group on metal-salen-based complexes. (bottom) Present work on metal-salen-based complexes derived from 8-formyl-7-hydroxycoumarin. *Please note: for clarity, axial ligand (H_2O or Cl^-) on metal-salen complexes is omitted.* [a]*Screening of metal cations was performed only with salen ligand based on 1,2-ethylenediamine (salen ligand **1**-**L**).*

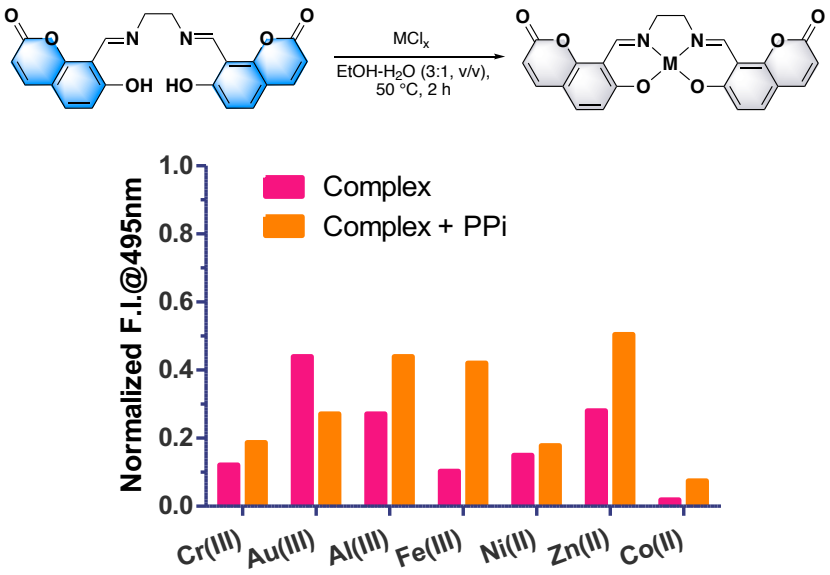

Fig. 3. Fluorescence response (Ex at 365nm, Em at 495 nm, Ex/Em bandwidths = 8 nm) of metal-salen complexes derived from **1-L** (10 μM) towards PPi anion (20 equiv.) in HEPES buffer (20 mM, pH = 7.2). Intensities normalized with respect to fluorescence emission of starting salen ligand **1-L.** *(top) Please note: depending on the metal cation source used, x = 2 or 3; for clarity, axial ligand (H_2O or Cl^-) on metal-salen complexes is omitted.*

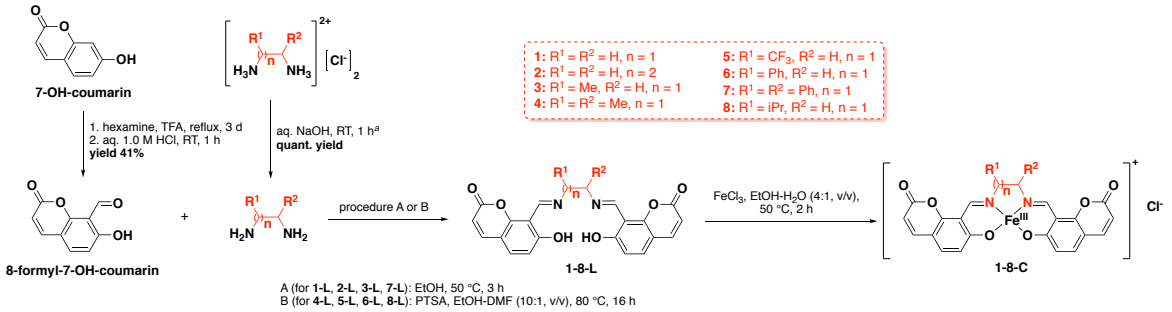

Entry	Vicinal diamine	Salen ligand yield (%)	Fe(III) complex yield (%)	Entry	Vicinal diamine	Salen ligand yield (%)	Fe(III) complex yield (%)
1		72%	32%	5	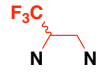	15%	22%
2		37%	56%	6	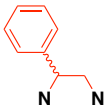	20%	18%
3		55%	43%	7	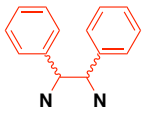	18%	3%
4		54%	30%	8	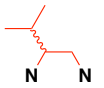	3%	56%

Scheme 1. Synthesis of coumarin-salen Fe(III) complexes (d = days, hexamine = hexamethylenetetramine, PTSA = *para*-toluenesulfonic acid, RT = room temperature). [a]*Some vicinal diamines (1,2-ethylenediamine, 1,3-diaminopropane, 1,2-propylenediamine and 1,2-diphenylethylenediamine) are commercially available directly as free base form and not subjected to this neutralization reaction. Please note: numbering of salen ligands and related Fe(III) complexes is based on entry's numbers of this table combined with letter "L" (for ligand) or "C" (for metal complex). A simplified representation of vicinal diamine molecules (column 2) was deliberately adopted in order to also illustrate the bridge of salen ligands and Fe(III) complexes. Please note: for clarity, axial ligand (H_2O or Cl^-) on metal-salen complexes is omitted.*

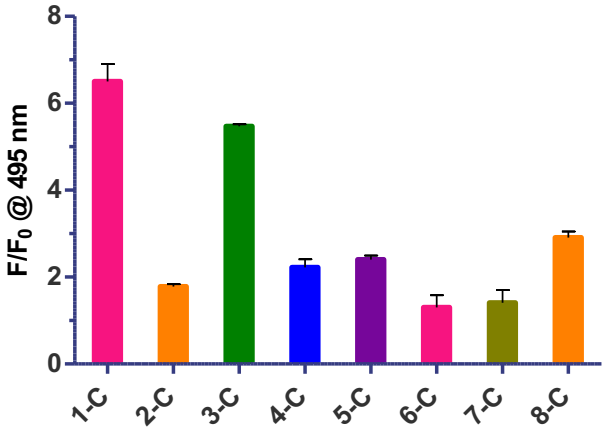

Fig. 4. Fluorescence response (Ex at 365nm, Em at 495 nm, Ex/Em bandwidths = 8 nm) of coumarin-salen Fe(III) complexes **1-C** to **8-C** (10 μM) towards PPi anion (20 equiv., incubation time = 60 min) in HEPES buffer (20 mM, pH = 7.2). Intensities normalized (F/F_0) with respect to residual fluorescence emission of metal complexes before PPi addition.

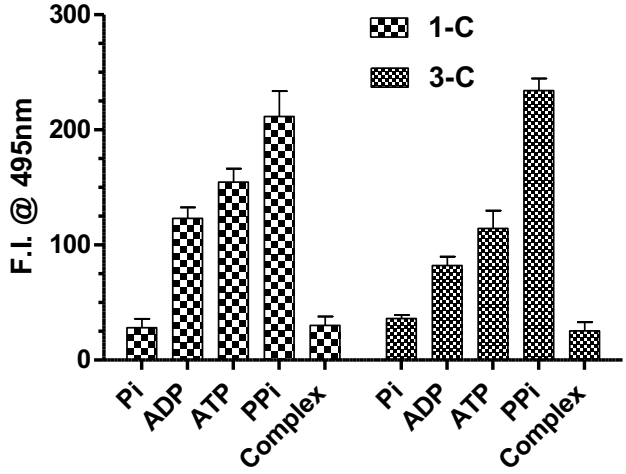

Fig. 5. Fluorescence response (Ex at 365nm, Em at 495 nm, Ex/Em bandwidths = 8 nm) of coumarin-salen Fe(III) complexes **1-C** and **3-C** (10 μM) towards (poly)phosphate species (20 equiv., incubation time = 60 min) in HEPES buffer (20 mM, pH = 7.2).

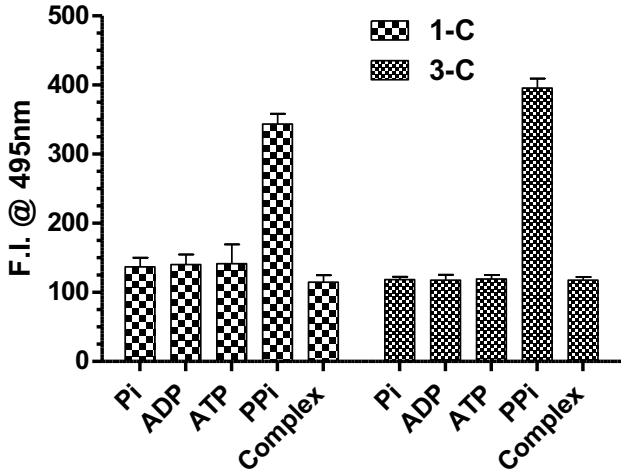

Fig. 6. Fluorescence response (Ex at 365nm, Em at 495 nm, Ex/Em bandwidths = 8 nm) of coumarin-salen Fe(III) complexes **1-C** and **3-C** (10 µM) towards (poly)phosphate species (20 equiv., incubation time = 60 min) in Tris.HCl buffer (20 mM, pH = 9.0).

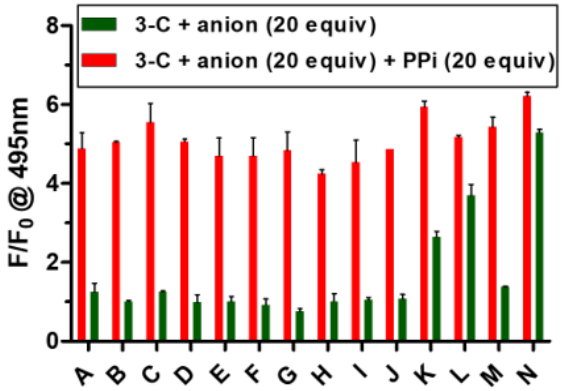

Fig. 7. Fluorescence response (Ex at 365nm, Em at 495 nm, Ex/Em bandwidths = 8 nm) of coumarin-salen Fe(III) complex **3-C** (10 µM) towards various anions (20 equiv., incubation time = 60 min) in HEPES buffer (20 mM, pH 7.2), analytes: A: NO_2^-, B: F^-, C: SCN^-, D: $CH_3CO_2^-$, E: HCO_3^-, F: CO_3^{2-} , G: Cl^- , H: Br^- , I: SO_4^{2-} , J: AMP, K: ADP, L: ATP, M: Pi, N: PPi. Intensities normalized (F/F_0) with respect to residual fluorescence emission of metal complexes before addition of the corresponding anionic analyte.

Table 1. Photophysical properties of 8-formyl-7-hydroxycoumarin, salen ligands and related Fe(III) complexes studied in detail for PPi detection, determined in HEPES (20 mM, pH 7.3) at 25 °C.

Cmpd[a]	λ Abs (nm)[b]	λ Em (nm)	ε (M^{-1} cm^{-1})	Stokes' shift (cm^{-1})	Φ_F (%)[c]
8-formyl-7-OH-coumarin	354	468	15 350	6 881	4
1-L	281, 349	510	25 350, 33 800	15 979, 9 045	1
1-C	354	465[d]	18 200	6 743	-[d]
3-L (fresh stock solution)	282, 349	477	23 200, 27 700	14 497, 7 689	2
3-L	282, 349	500	-[e]	15 461, 8 653	1
3-C	359	462[d]	23 250	6 210	-[d]

[a] stock solutions (1.0 mg/mL) were prepared in spectroscopic grade DMSO.
[b] a shoulder close to 400 nm was also observed for salen ligands.
[c] determined using 7-hydroxycoumarin as standard (Φ_F = 76% in phosphate buffer (100 mM, pH 7.4), Ex at 340 nm) [31]. Relative fluorescence quantum yield of 7-hydroxycoumarin was also determined in HEPES buffer (20 mM, pH 7.3), Φ_F = 84%.
[d] residual fluorescence emission was observed only with concentrated solutions (ca. 20 mM) and thus it was not possible to determine a relative fluorescence quantum yield (too low value). Both Fe(III) complexes can be assumed as non-fluorescent.
[e] prolonged storage of stock solution at 4 °C, and repeated freeze-thaw cycles led to partial precipitation and changes in emission maximum and fluorescence quantum yield.

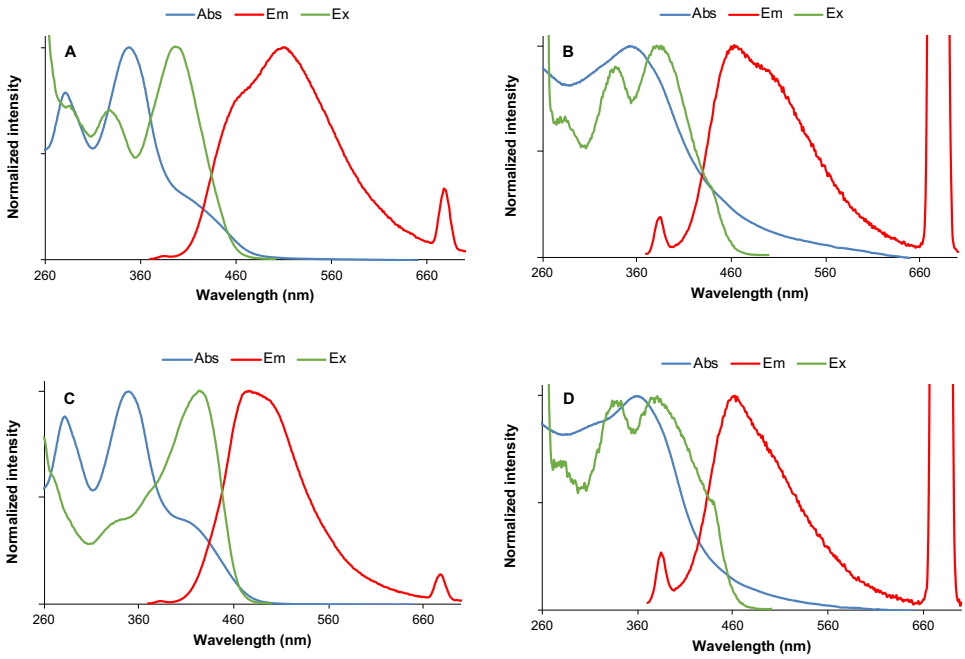

Fig. 8. Normalized UV-visible absorption (blue), fluorescence emission (Ex at 340 nm, Ex/Em slits = 5 nm, red) and excitation (Em at 520 nm, Ex/Em slits = 5 nm, green) spectra of **1-L** (A), **1-C** (B), **3-L (fresh stock solution)** (C), and **3-C** (D) in HEPES buffer, at 25°C. *Please note: for the emission spectra, peaks at 385 nm and 680 nm (2x λEx) corresponds to Stokes Raman scattering peak of water, and Rayleigh scattering peak respectively.*

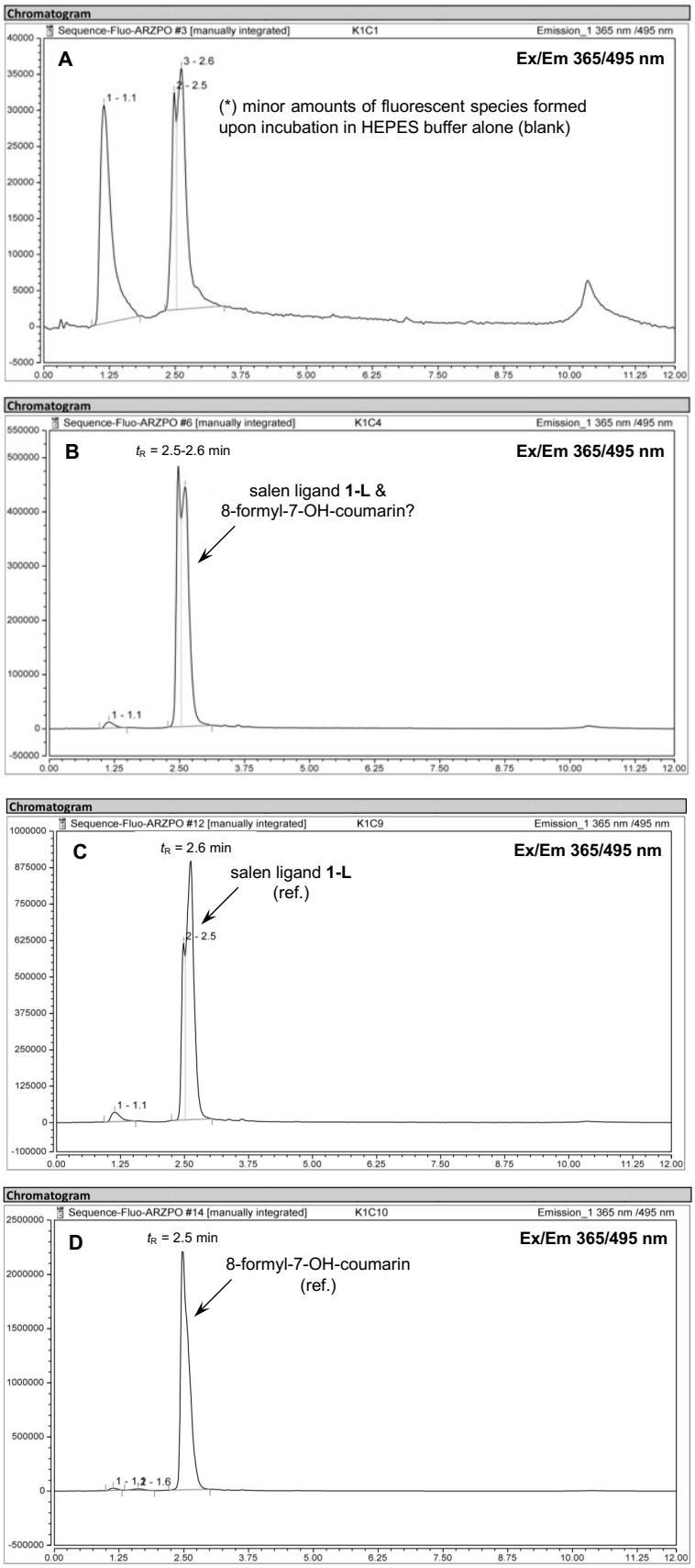

Fig. 9. RP-HPLC elution profiles (system A, fluorescence detection at Ex/Em 365/495 nm) of Fe(III)-salen complex **1-C** after incubation in HEPES buffer (20 mM, pH 7.3) for 2 h at 25 °C, without PPi (A) and with 20 equiv. of PPi (B); salen ligand **1-L** (C) and 8-formyl-7-hydroxycoumarin (D) after incubation in HEPES buffer alone.